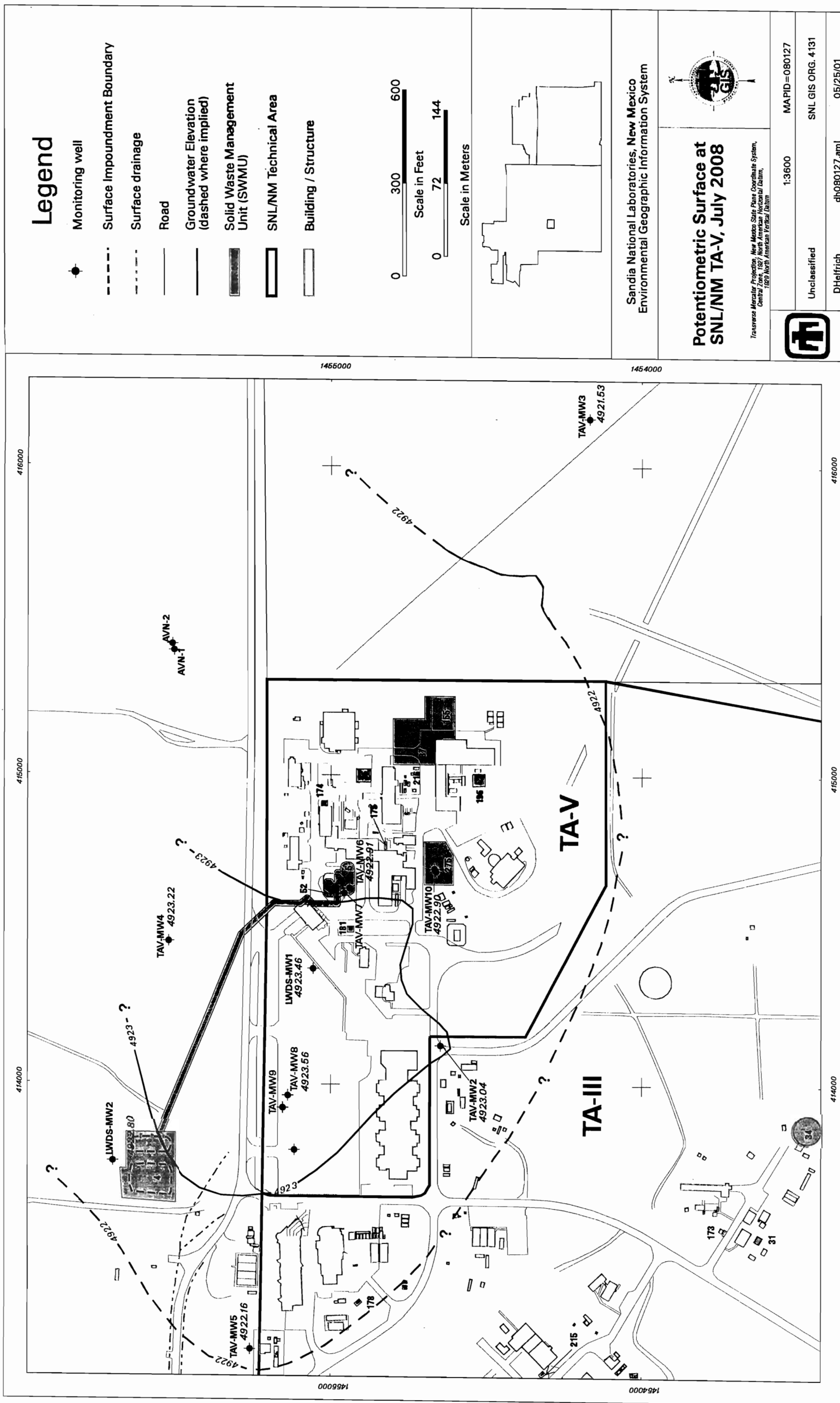


AGENDA
NMED, DOE, and SNL/NM MEETING
SEPT 18, 2008

Agenda Item 1: TA-V Groundwater Characterization

Topic	Handouts
Per the NOD Comments, the well network has been resurveyed.	<ul style="list-style-type: none"> ◆ Table with well measuring point elevations (old and new). ◆ Site-specific potentiometric surface map with recent water level measurements and revised elevations). ◆ Subregional potentiometric surface map. ◆ Water levels versus time for select wells (uncorrected for new measuring point elevations).
TCE concentrations as of July 2008.	<ul style="list-style-type: none"> ◆ TCE 2003 distribution map. ◆ TCE 2008 distribution map. ◆ TCE versus time plot for wells with detectable concentrations. ◆ Draft of the most recent numerical model (prepared in 2006 in support of an internal draft of the CMIP as Appendix C).
Nitrate concentrations as of July 2008.	<ul style="list-style-type: none"> ◆ Nitrate 2008 distribution map. ◆ Nitrate versus time plot for LWDS-MW1.

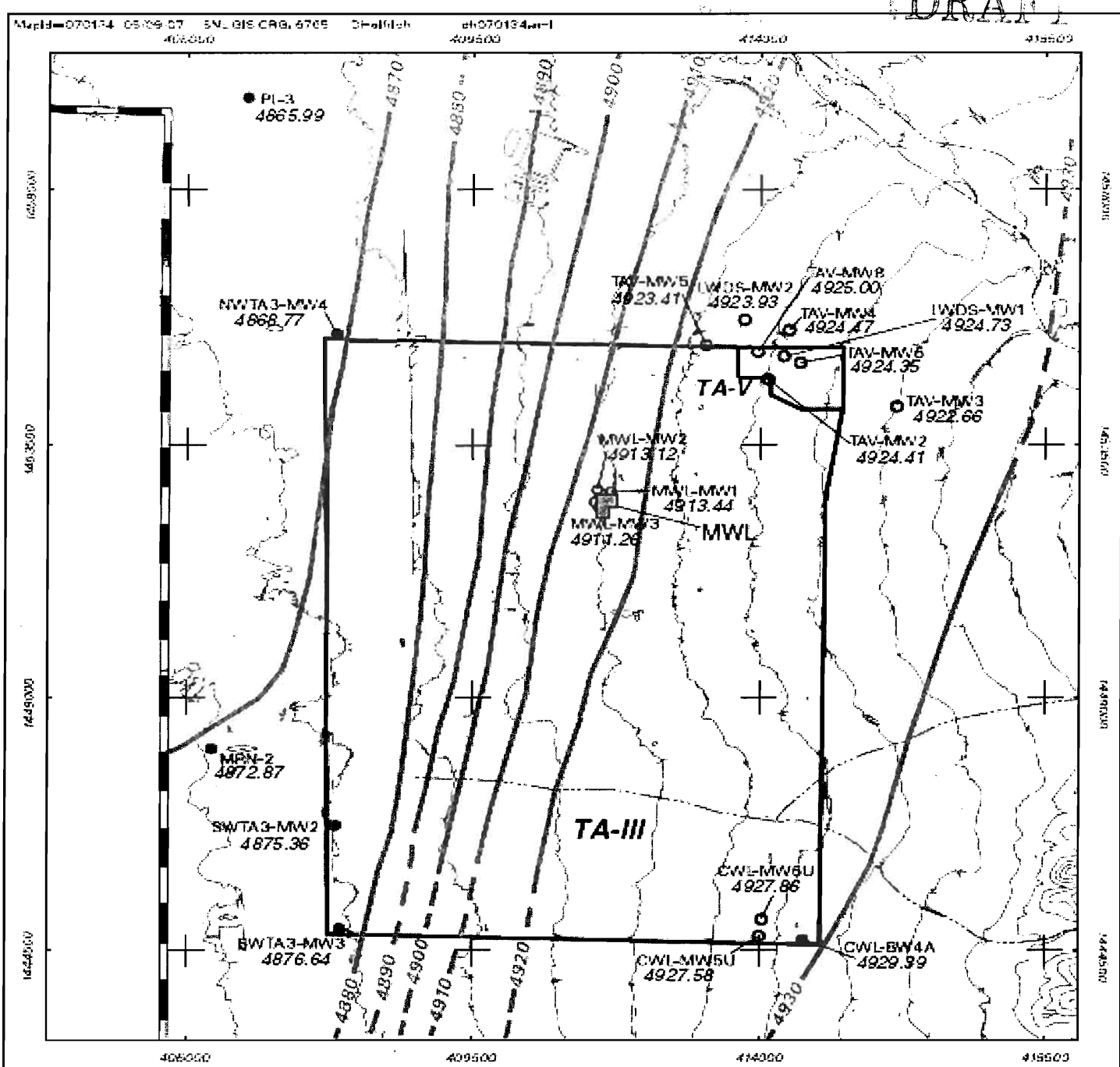
Agenda Item 2: Proceeding Towards Completing Characterization and Implementing the Corrective Measure



Summary of Old and New TA-V Well Survey Data (New Survey Completed September 2008),
and New Water Level Elevations

Well ID	Old Measuring Point Elevation (FAMSL)	New Measuring Point Elevation (FAMSL)	Difference (new - old)	Measured Depth to Water (FBTOC, July 1-9, 2008)	New Water Level Elevation (FAMSL)
AVN-1	5440.55	5440.27	-0.28	519.44	4920.83
LWDS-MW1	5422.19	5421.05	-1.14	497.59	4923.46
LWDS-MW2	5409.81	5409.68	-0.13	486.88	4922.80
TAV-MW2	5424.86	5424.6	-0.26	501.56	4923.04
TAV-MW3	5461.73	5461.53	-0.2	540.00	4921.53
TAV-MW4	5425.39	5425.16	-0.23	501.94	4923.22
TAV-MW5	5406.20	5405.98	-0.22	483.82	4922.16
TAV-MW6	5428.74	5428.44	-0.3	505.53	4922.91
TAV-MW7	5428.00	5427.67	-0.33	508.08	4919.59
TAV-MW8	5414.55	5414.27	-0.28	490.71	4923.56
TAV-MW9	5413.83	5413.54	-0.29	494.52	4919.02
TAV-MW10	5434.30	5434.30	0	511.40	4922.90

FAMSL = Feet above mean sea level.
FBTOC = Feet below top of casing (measuring point, north side of PVC casing)



Legend

- Monitoring Well (groundwater elevation measured Jan. 2007, feet above mean sea level)
- Monitoring Well (groundwater elevation measured March 2007)
- Monitoring Well (groundwater elevation measured April 2007)
- Monitoring Well (groundwater elevation measured Oct. 2006)

20-foot Ground Surface Contour Interval



Kirtland Air Force Base Boundary



Potentiometric Surface Contour
(feet above mean sea level, dashed where approximate)



Technical Area

MWL - Mixed Waste Landfill

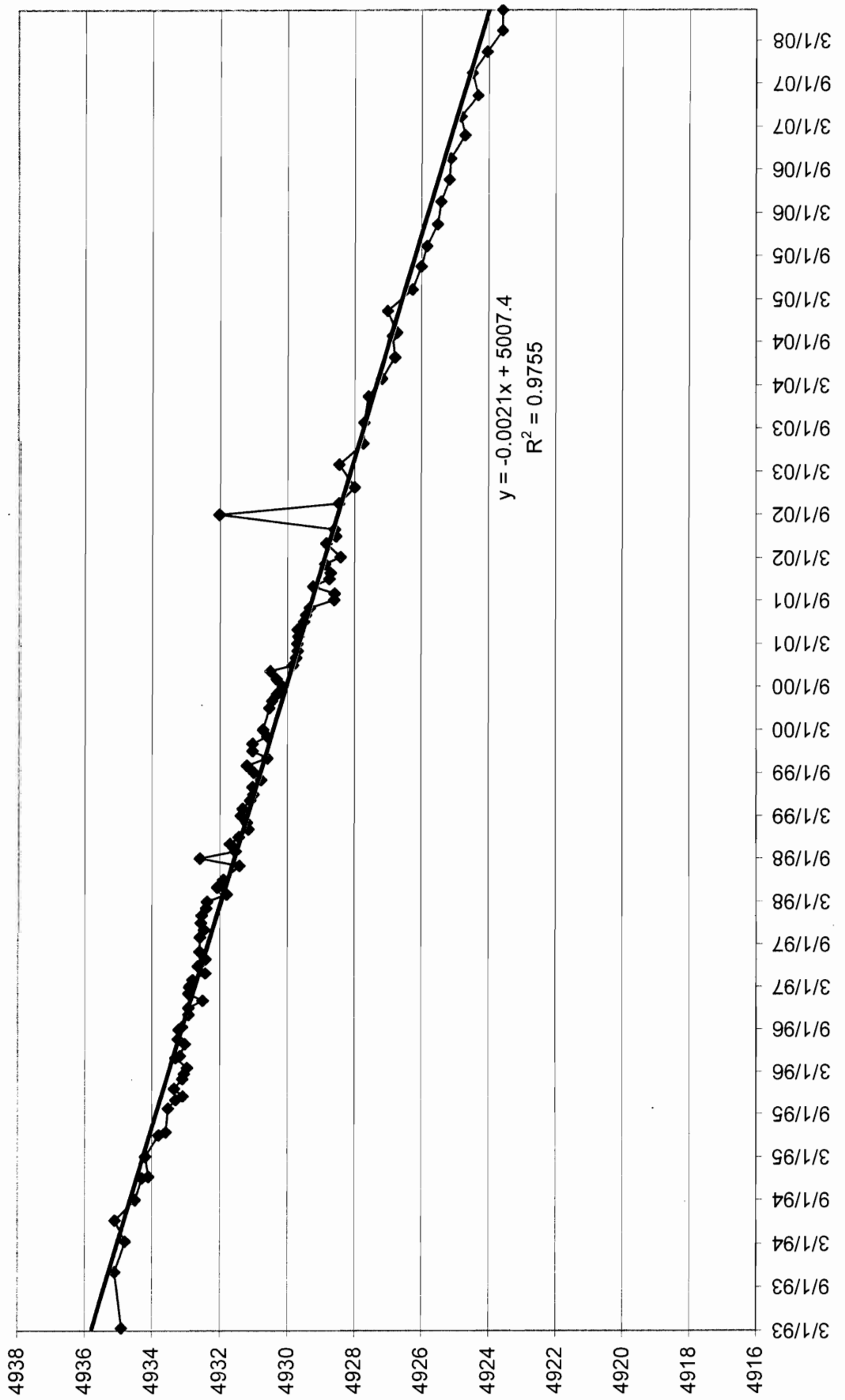
Sandia National Laboratories, New Mexico

**Sandia National Laboratories, New Mexico
Environmental Geographic Information System**

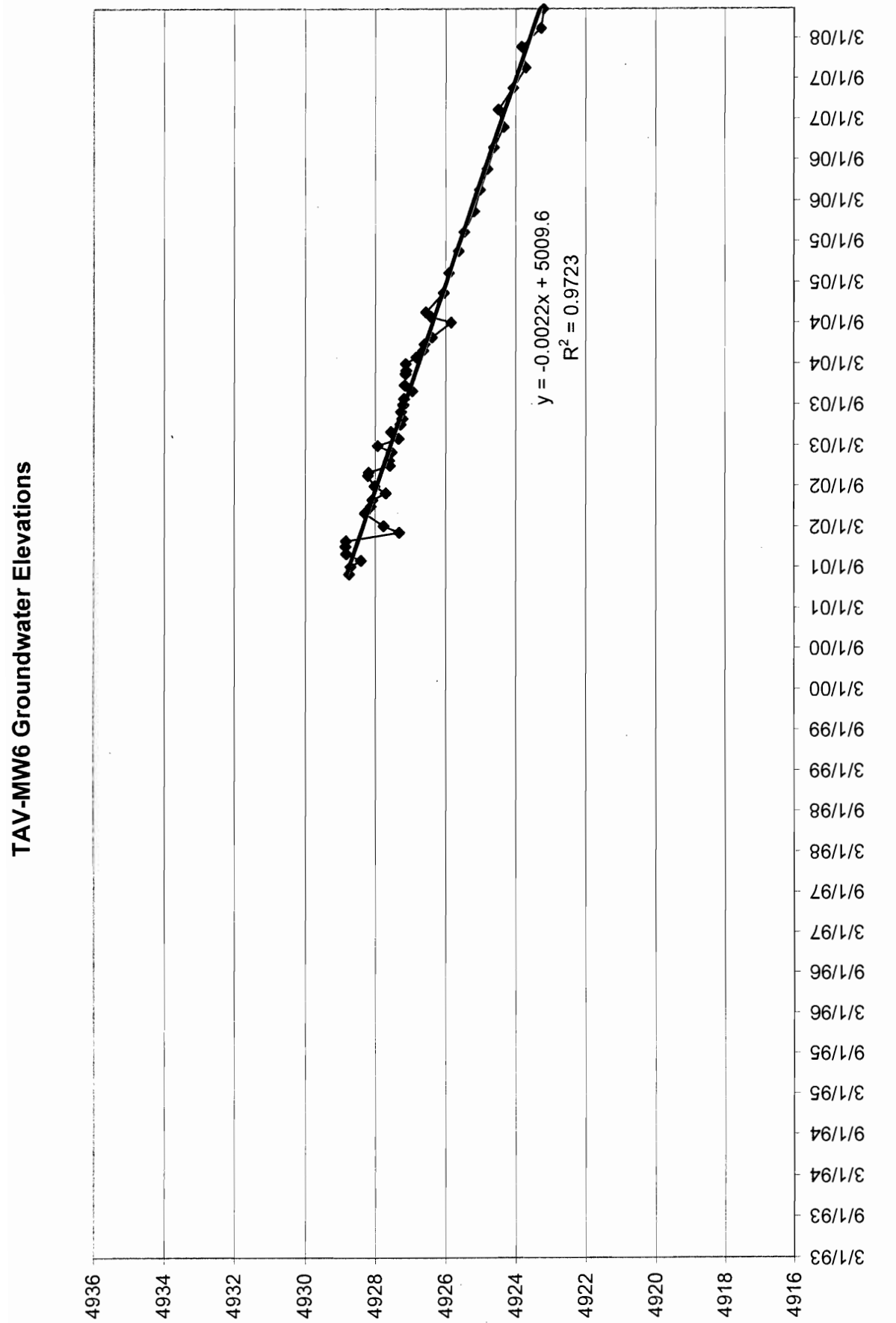
640857.04300000 A4

Figure 4.1-2 Localized Potentiometric Surface of Basin Fill Aquifer at Technical Area III

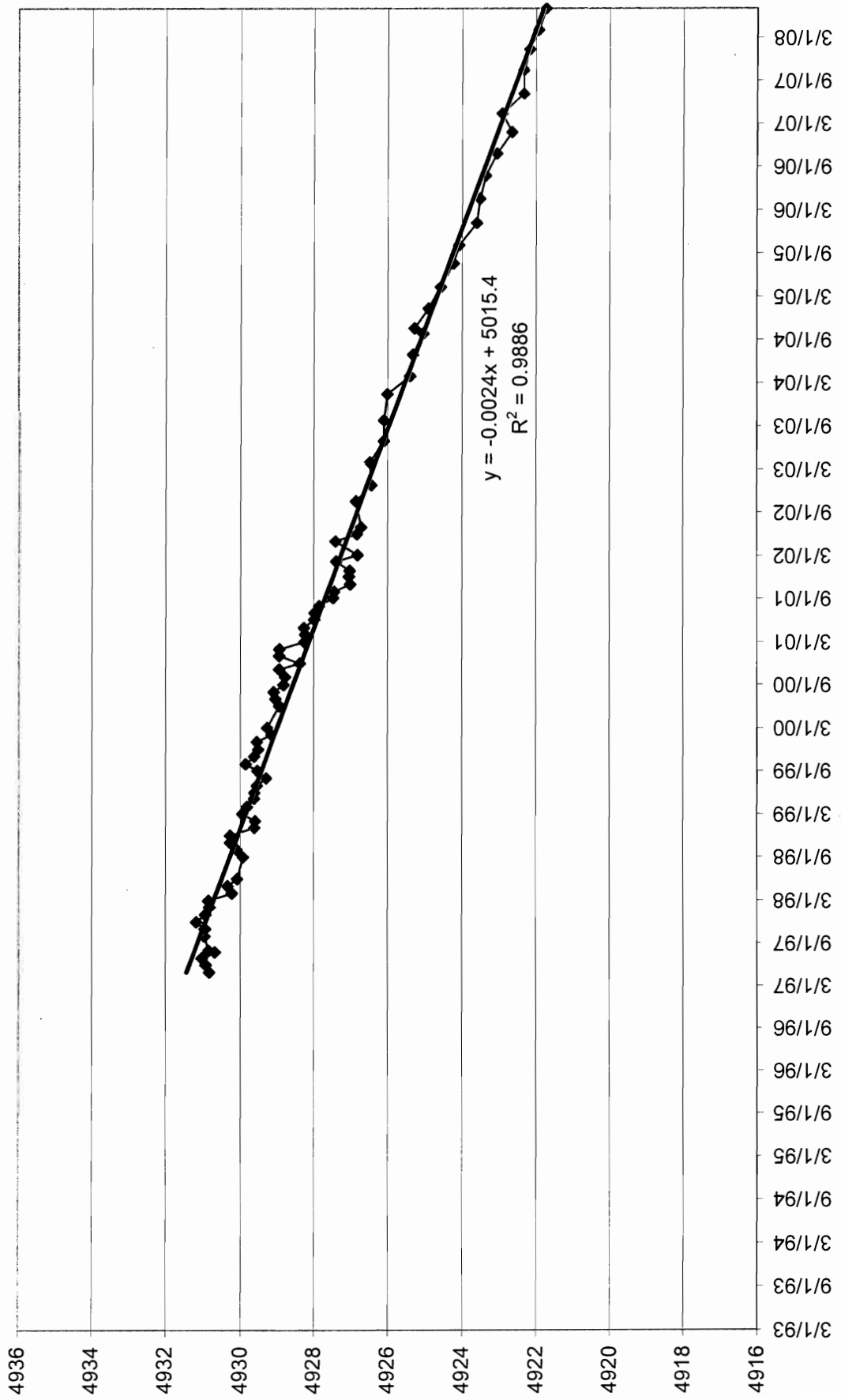
LWDS-MW1 Groundwater Elevations



TAV-MW6 Groundwater Elevations



TAV-MW3 Groundwater Elevations



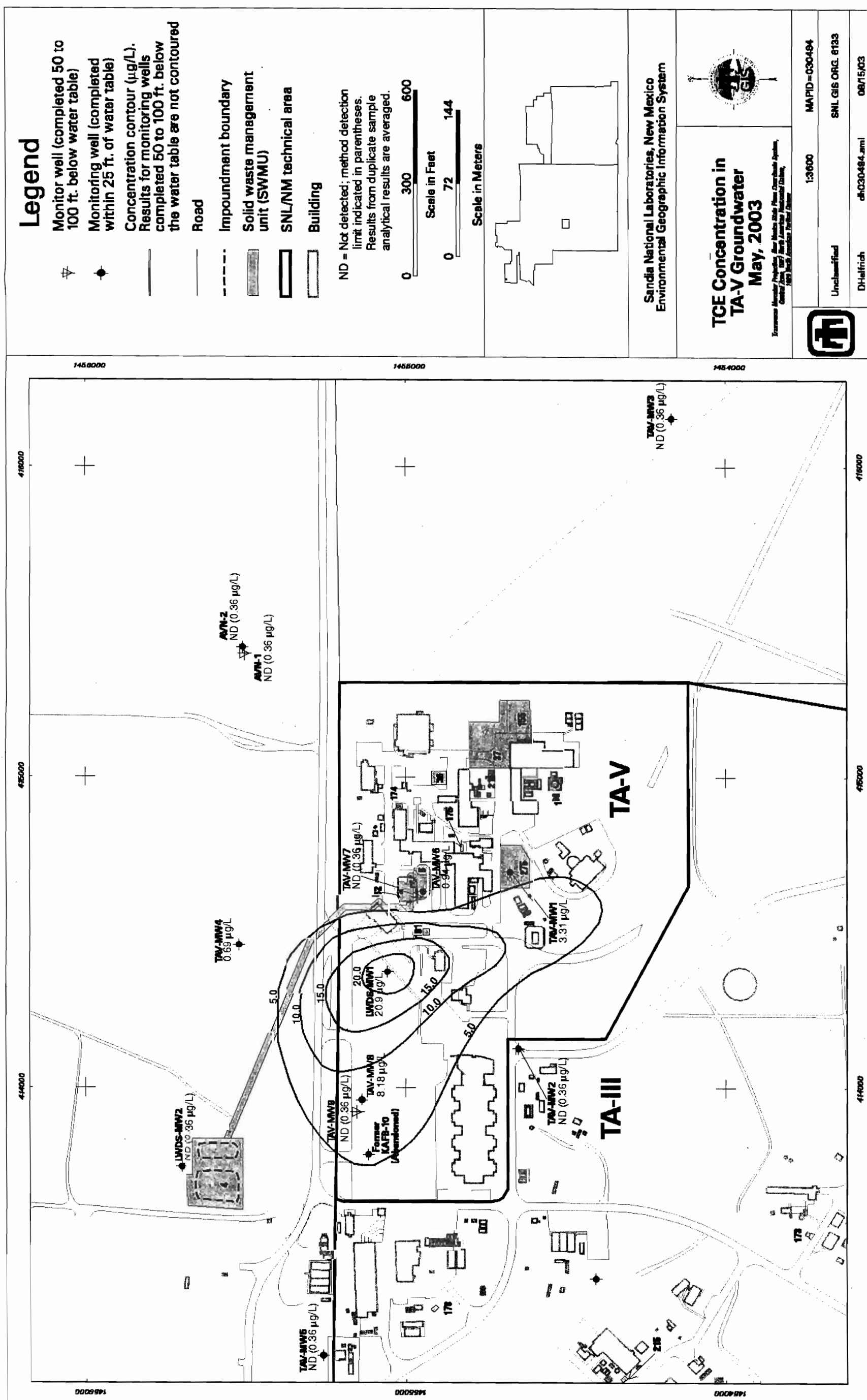
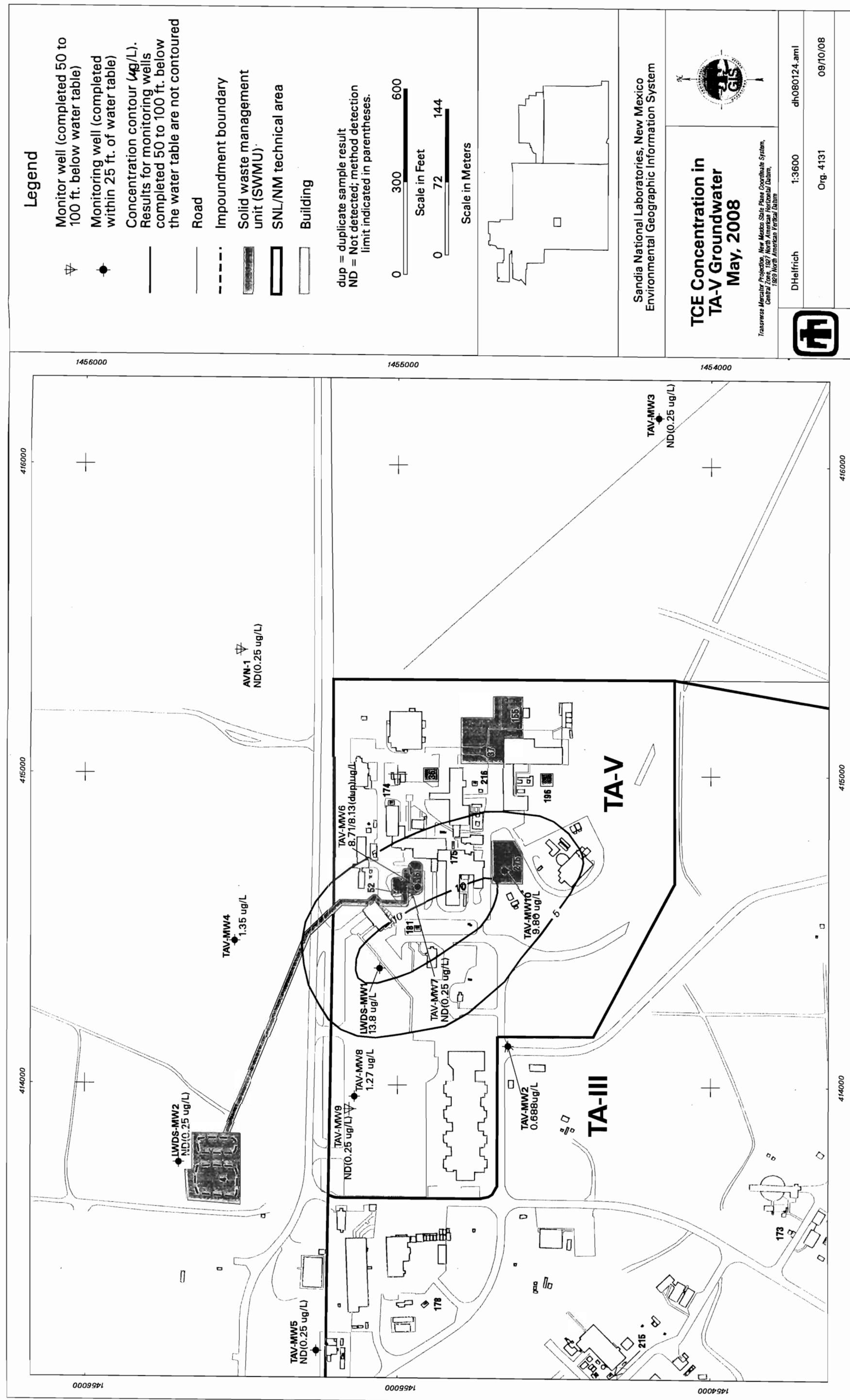
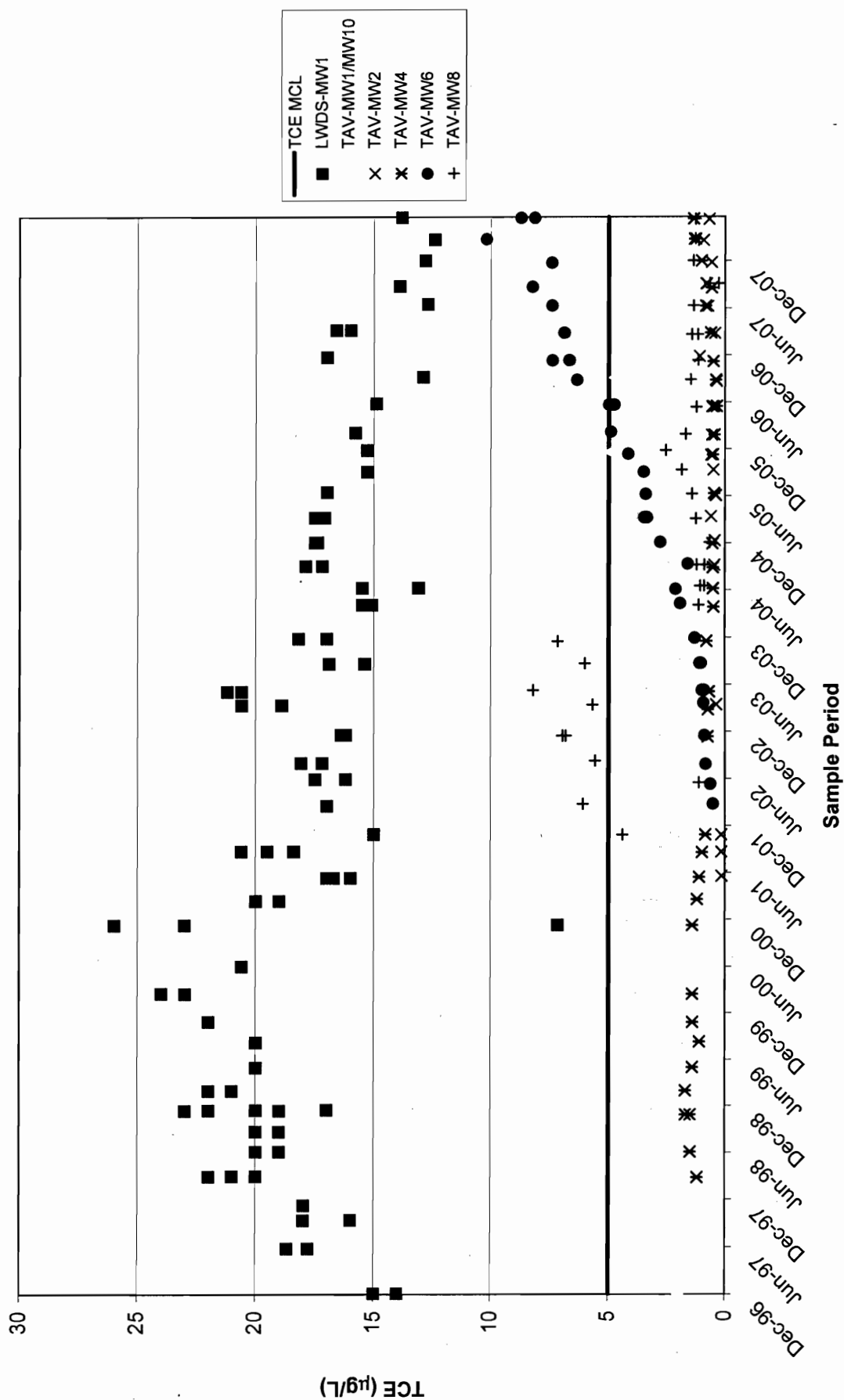
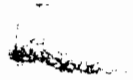


Figure 1-2. Location of the TCE plume within the TA-V area.





Corrective Measures Implementation Plan for Technical Area-V Groundwater (DRAFT)

 **DRAFT**

Jonathan L. Witt; Kevin A. Hall;
Ann O'Hagan; Dana L. Dettmers; M. Hope Lee
North Wind, Inc.
Idaho Falls, Idaho

Abstract

This Corrective Measures Implementation Plan identifies the approach and requirements for implementing monitored natural attenuation (MNA) as the corrective measure for remediation of trichloroethene, tetrachloroethene, and nitrate in groundwater at Technical Area-V at Sandia National Laboratories/New Mexico. This plan was prepared as directed by a Compliance Order on Consent issued by the New Mexico Environment Department to outline the strategy, operations and maintenance requirements, evaluation and reporting requirements, project team qualifications, and schedule for implementing the MNA remedy. This document also provides information supporting the implementation of the MNA remedy, and the MNA remedy goals and objectives.

ATTACHMENT C

Groundwater Flow and TCE Transport Model for
Technical Area-V and Vicinity

DRAFT

DRAFT

This Page Intentionally Left Blank

DRAFT

Abstract

Numerical modeling was performed to support implementation of the monitored natural attenuation corrective measure for Technical Area-V groundwater. This modeling activity provides a local-scale simulation of groundwater flow and trichloroethene transport and attenuation in the upper region of the aquifer where trichloroethene contamination is present. The numerical model is based on the current conceptual model of groundwater flow and contaminant transport and incorporates local heterogeneities in hydrogeologic properties, advection, dispersion, and biological degradation. The model results illustrate that, during implementation of the remedy, plume dynamics will be governed by local heterogeneities, which result in radial groundwater flow at velocities that are slower than subregional flow. Natural attenuation processes, such as biological degradation and dispersion, will act to decrease concentrations before significant migration of trichloroethene away from monitoring wells occurs. Natural attenuation processes are expected to reduce trichloroethene concentrations to below cleanup goals by the year 2049, with a 95% confidence interval corresponding to the years 2032 and 2120.

DRAFT

This Page Intentionally Left Blank

Contents

DRA

C-1. PURPOSE.....	C-9
C-1.1 Summary of CME Modeling	C-9
C-2 CMI MODEL DESCRIPTION.....	C-10
C-2.1 Model Domain	C-16
C-2.2 Model Calibration.....	C-17
C-3 RESULTS AND INTERPRETATION	C-20
C-3.1 Local Groundwater Flow Characteristics	C-20
C-3.2 Future TCE Plume Dynamics	C-21
C-3.3 Achieving Cleanup Goals	C-25
C-4. IMPLICATIONS FOR CORRECTIVE MEASURES IMPLEMENTATION	C-27
C-5. REFERENCES	C-28
Appendix A. Simulated and Observed Head at Selected Wells	C-29
Appendix B. Simulated and Observed TCE Concentrations at Selected Wells	C-39

Figures

C-1. Model grid illustrating model boundaries and discretization.	C-16
C-2. Simulated hydraulic conductivity distribution.....	C-18
C-3. Simulated potentiometric surface in 2006.	C-19
C-4. Simulated groundwater flow vectors near TA-V (2001).	C-21
C-5. Simulated TCE concentration contours using the average degradation rate constant. .	C-22
C-6. Simulated TCE concentration contours using the upper 95% confidence interval of the degradation rate constant.	C-23
C-7. Simulated TCE concentration contours using the lower 95% confidence interval of the degradation rate constant.	C-24

Tables

C-1. Conceptual Model Elements and Application to Numerical Model.....	C-11
------------------------------------------------------------------------	------

DRAFT

This Page Intentionally Left Blank

Acronyms and Abbreviations

DRAFT	
amsl	above mean sea level
ARG	ancestral Rio Grande
CME	Corrective Measures Evaluation
CMI	Corrective Measures Implementation
COA	City of Albuquerque
COC	contaminant of concern
EPA	U.S. Environmental Protection Agency
ft	feet
GMS	Groundwater Modeling System
KAFB	Kirtland Air Force Base
LWDS	liquid waste disposal system
MCL	maximum contaminant level
mi ²	square miles
MNA	monitored natural attenuation
MODFLOW	Modular Three Dimensional Groundwater Flow Model
PCE	tetrachloroethene
PEST	parameter estimation
SNL/NM	Sandia National Laboratories/New Mexico
TA	technical area
TCE	trichloroethene
µg/L	micrograms per liter

DRAFT

This Page Intentionally Left Blank

C-1. PURPOSE

Numerical modeling was performed to support implementation of the monitored natural attenuation (MNA) corrective measure for Technical Area-V (TA-V) groundwater. The model builds on earlier numerical modeling activities (summarized in Section C-1.1) that supported the Corrective Measures Evaluation (CME), as described in the “Corrective Measures Evaluation Report for Technical Area-V Groundwater” (SNL/NM 2005). The CME numerical modeling activity provided a conservative estimate of the potential for contaminant migration to receptors on a sub-regional scale. The Corrective Measures Implementation (CMI) model incorporates a local groundwater flow model with heterogeneities, advection, dispersion, and biological degradation into a simulation of trichloroethene (TCE) transport and natural attenuation processes.

The CMI model was performed to support implementation of the MNA remedy by providing a local-scale simulation of groundwater flow and TCE transport and attenuation in the upper region of the aquifer where TCE contamination is prevalent. TCE has been detected in several TA-V monitoring wells, as presented in Attachment A. The CMI model primarily applies to TCE, which is one of three contaminants of concern (COCs) at the site. Tetrachloroethene (PCE) and nitrate have been detected in some wells at the site, and are less widely distributed than TCE. The numerical modeling provided useful information for CMI in regards to TCE because of the distribution of TCE and nature of the degradation mechanism. Application of MNA for all three COCs can be protective and meet cleanup goals based on the information presented in the CME report (SNL/NM 2005).

C-1.1 Summary of CME Modeling

Numerical modeling activities were performed to support evaluation of corrective measures for TA-V, as described in the TA-V CME Report (SNL/NM 2005). A United States Geological Survey regional numerical model of groundwater flow was initially adapted to evaluate contaminant dilution in groundwater downgradient from TA-V (Written Communication, Greg Ruskauf, INTERA Inc., November 10, 2004). The objective of this analysis was to determine the reduction in dissolved concentration of contaminants (i.e., TCE) derived from TA-V sources as those contaminants migrate in groundwater that is drawn toward the capture zone of City of Albuquerque (COA) municipal well fields. Analysis of these regional numerical model results showed that the discretization of the regional model was too large for the scale of the TA-V contaminant dilution problem. A simplified cross-sectional analysis was developed to refine estimates of downgradient dilution of a conservative contaminant.

The objective of the cross-sectional analysis was to conservatively evaluate the potential for transport of contaminants to production wells, which in the case of the COA’s Ridgecrest water supply wells, are located approximately six miles downgradient of TA-V. Production wells considered included existing wells operated by the COA and Kirtland Air Force Base (KAFB) and a hypothetical production well, which was included in order to evaluate the potential for transport of contaminants to the proposed Mesa del Sol wells. Although this hypothetical production well was considered, the proposed Mesa del Sol production wells are not expected to be receptors of contamination originating from TA-V, as explained in the CME Report (SNL/NM 2005).

The results of the CME modeling activity support the decision to apply MNA for TA-V groundwater. Contaminant concentrations were predicted to decline almost four orders of

DRAFT

magnitude before reaching production wells, and to be far below the maximum concentration allowed in drinking water (i.e., maximum contaminant levels [MCLs]). The model also predicted a travel time of at least 230 years before contaminants would reach the Ridgecrest wells at reduced concentrations.

Anomalously low hydraulic conductivity in the vicinity of TA-V and the effects of biological degradation, sorption, decay, and lateral dispersion were intentionally neglected in the CME model to provide a conservative overestimation of contaminant concentrations and rate of contaminant migration to production wells. The scale of the groundwater model (several miles) and intentional neglect of some processes that would further reduce contaminant concentrations provided a conservative evaluation of the potential for migration of contaminants to production wells. However, the CME model does not provide a sufficiently accurate representation of contaminant transport for the CMI because it was not intended to represent distribution of contaminants on the smaller scale representative of TA-V and its vicinity. The CME model also did not account for biological degradation of TCE. The more refined model for the TA-V area described here was developed to predict TCE degradation and transport near TA-V to support development of the CMI Plan.

The results of both the CME and CMI modeling activities were used to devise the MNA implementation strategy. The results of the CME numerical modeling activity were used to devise action levels, which are performance metrics (as described in Section 2-4 of the CMI Plan). The results of this CMI numerical modeling activity are used to develop the groundwater monitoring strategy and provide an estimate of the remedy implementation timeframe.

C-2 CMI MODEL DESCRIPTION

A numerical model was created to represent groundwater flow and TCE transport in the subsurface at and near TA-V. The model utilized the Department of Defense Groundwater Modeling System (GMS), employing the Modular Three Dimensional Groundwater Flow Model (MODFLOW) groundwater flow simulator (Harbaugh et al. 2000) and the MT3DMS transport simulator (Zheng and Wang 1999) with GMS pre- and post-processors (BYU 2003).

The conceptual basis for the development of this numerical model is described in the “Current Conceptual Model of Groundwater Flow and Contaminant Transport at Sandia National Laboratories/New Mexico Technical Area-V” (SNL/NM 2004). In addition, assumptions and input values from previous numerical models of this groundwater system were used. These included work described in the TA-V CME Report (SNL/NM 2005) and the following documents:

- “Simulated Effects of Ground-Water Management Scenarios on the Santa Fe Group Aquifer System, Middle Rio Grande Basin, New Mexico, 2001-40” (Bexfield and MacAda 2003), and
- “SNL/NM Environmental Restoration Project Long-Term Monitoring Strategy for Groundwater” (SNL/NM 2001).

Table C-1 lists physical observations and conceptual model elements and presents how each of these elements was incorporated into the numerical simulation by input of parameter values and assumptions. Additional detail provided in this section includes a description of the model domain (Section C-2.1) and calibration methods (Section C-2.2).

Table C-1. Conceptual Model Elements and Application to Numerical Model

Conceptual Model Element	Physical Description	Numerical Representation
Regional Aquifer Properties	<p>Extent – The Santa Fe Group aquifer encompasses approximately 3,000 mi² of the Albuquerque Basin. Groundwater flow at TA-V occurs entirely within deposits of the Santa Fe Group aquifer.</p> <p>Hydrostratigraphy – Regionally, stratigraphic units consist of alluvial fan/piedmont deposits derived from uplifts adjacent to the Albuquerque Basin and ancestral Rio Grande (ARG) deposits transported from upstream basins north of TA-V. Alluvial fan/piedmont deposits range in texture from clays to coarse gravel and cobbles. Deposits locally are lenticular and highly variable in distribution and thickness. Close to mountain fronts, deposits are coarse grained and poorly sorted. Basinward, deposits become finer grained and better sorted. Alluvial fan/piedmont deposits comprise sediments at TA-V.</p>	<p>The numerical model is a simulation of TA-V and its local vicinity, which is primarily within the alluvial fan/piedmont deposits. Regional hydrogeologic characteristics are incorporated into the numerical simulation as boundary effects and hydrogeologic properties that are described in greater detail below.</p>
Layering		<p>Predominantly Horizontal Flow - The lenticular layered nature of the alluvial fan sediments results in predominantly horizontal flow. Previous simulations have used a horizontal to vertical hydraulic conductivity ratio of 150:1 (SNL/NM 2005).</p> <p>Lithology – In general, grain size in the alluvial fan deposits decreases with depth. Generalized lithology derived from drilling logs from KAFB-10, an abandoned supply well, show a lower permeability unit located approximately 50 ft below the current water level. This well was located within the boundary of TA-V. The generalized lithology illustrates the layered nature of the alluvial fan deposits at TA-V and the presence of low permeability clay layers.</p> <p>TCE is Not Found in Deeper Portion of the Aquifer - TCE has not been observed in the deep wells, TAV-MW9 and TAV-MW7 (although minor amounts of PCE have been detected in TAV-MW7, as described in Attachment A).</p>

Table C-1 (continued)

Conceptual Model Element	Physical Description	Numerical Representation
Inflows	<p>Mountain Front and Intermittent Tributary Recharge – Runoff from mountainous drainage basins that are tributary to the Albuquerque Basin recharges the Santa Fe Group aquifer as infiltrating ephemeral streamflows along arroyo channels and as underflow moving into the Santa Fe Group from bedrock boundaries. Infiltrating streamflow and groundwater underflow into the Santa Fe Group aquifer along the mountain front east of TA-V constitute the predominant sources for groundwater in the vicinity of TA-V.</p> <p>Recharge from Direct Precipitation – The average precipitation at Albuquerque is less than nine inches per year, more than half of which occurs during July through October as thundershowers. Potential evaporation losses may be as much as 10 times precipitation. Recharge from direct precipitation is considered to be negligible.</p> <p>Other Sources of Recharge – Regionally, streamflow and irrigation from the Rio Grande constitutes the bulk of recharge to the aquifer. This source of recharge does not directly affect groundwater flow in the vicinity of TA-V. Recharge from septic systems constitutes a minor source of recharge in the basin. Historically at TA-V, wastewater disposals to drainfields, surface impoundments, and seepage pits have locally provided sources of recharge to the aquifer. These sources of recharge at TA-V have ceased.</p>	<p>Mountain front recharge occurs east of the TA-V model domain. The effect of recharge from infiltration and bedrock underflow is numerically represented by a specified head boundary on the east side of the model domain. This boundary is represented by water level observations in wells CWL-BW4A and KAFB-6301 over time.</p> <p>Recharge from infiltration of precipitation and other sources is not numerically represented because they are considered to be negligible within the model domain.</p>

Table C-1 (continued)

Conceptual Model Element	Physical Description	Numerical Representation
Outflows	<p>Regional Outflow – Natural outflows from the Santa Fe Group aquifer include losses to streamflow and evaporation along the present day Rio Grande channel and groundwater underflow out of the Albuquerque Basin into downstream basins.</p> <p>Groundwater Withdrawals – Withdrawals from municipal well fields located in Albuquerque, KAFB production wells, and Veterans Administration Hospital production wells constitute a major outflow from the Santa Fe Group aquifer. These withdrawals have created a large cone of depression in the water table and have effectively changed the direction of groundwater flow relative to pre-development conditions.</p> <p>Other Outflows – Local pumping withdrawals have been minimal. The KAFB-10 pumpage was for fire suppression and was abandoned in April 1996.</p> <p>Declining Water Levels – The entire region is characterized by falling water levels. Water levels are continuously declining within the Albuquerque Basin because groundwater withdrawal rates exceed recharge rates. Seasonal variations in withdrawals are effectively damped out near TA-V.</p>	<p>Aquifer outflows occur outside of the model domain. The effect of the regional outflows on the aquifer within the model domain is incorporated as the western specified head boundary, which simulates head in the wells NWTA3-MW2, MRN-2, and a trend similar to those observed in PL-3.</p> <p>Sub-regional and regional water level declines due to pumping are assumed to continue into the future at the same rate as has been observed at the various well locations. Therefore, it is assumed that the rate of pumping over the simulated timeframe will not change significantly.</p> <p>Although all water levels with their corresponding month and year were used in model calibration, the resulting flow model effectively dampens seasonal variation in water levels.</p>

Table C-1 (continued)

Conceptual Model Element	Physical Description	Numerical Representation
Hydraulic properties	<p>Within the vicinity of TA-V, the aquifer material is composed of alluvial fan/piedmont deposits that are lenticular in nature and may be highly heterogeneous. Potentiometric surface maps for TA-V groundwater indicate the presence of a subtle groundwater mound, which is considered to be an artifact of regional water level declines within a heterogeneous aquifer.</p> <p>In general, the following values are reasonable and have been used in previous simulations to represent hydraulic properties:</p> <ul style="list-style-type: none"> • Hydraulic conductivity within the alluvial deposits ranges from 0.01 to 35 ft/day (SNL/NM 2004), • Specific yield is 0.18 (SNL/NM 2001), • Specific storage is $2 \times 10^{-6} \text{ ft}^{-1}$ (Bexfield and MacAda 2003), and • Porosity is 0.25 (SNL/NM 2005). 	<p>Automated parameter estimation (PEST) was used to calibrate the flow model to observed heads. The horizontal hydraulic conductivity was limited to a range of 0.01 to 35 ft/day.</p> <p>Specific yield, specific storage, and porosity were set at constant values throughout the model domain.</p>
TCE degradation	<p>Laboratory studies indicate that TCE degradation in the field will occur at a rate described by the first-order rate constant of $9.6 \times 10^{-5} \text{ days}^{-1}$, with a 95% confidence interval of $\pm 5.8 \times 10^{-5} \text{ days}^{-1}$.</p>	<p>Using first-order degradation kinetics to simulate degradation, the MT3DMS model was run three times using the average degradation rate constant and the upper and lower 95% confidence limits.</p>

Table C-1 (concluded)

Conceptual Model Element	Physical Description	Numerical Representation
Current TCE distribution	<p>TCE was present in wastewater disposed to the liquid waste disposal system (LWDS) drainfield and the TA-V seepage pits, which are shown on Figure 2-1 of the CMI Plan. This wastewater moved through the vadose zone and into groundwater. A dilute lobe of the TCE plume occurs south of well L-WDS-MW1 and west of the TA-V seepage pits. This lobe is attributed to TCE originating from the seepage pits that was subsequently diluted by continued discharges to the pits after TCE disposal ceased. Distribution of TCE from this source is attributed to dilution and attenuation. Disposals of TCE-contaminated wastewater to these probable sources has ceased.</p>	<p>The following four elements were considered when specifying initial concentrations in the model:</p> <ol style="list-style-type: none"> 1. The locations of potential sources of contamination on the surface, 2. Disposal history, including dilution of TCE during continued disposal of wastewater without TCE, 3. Concentration trends in TA-V wells, 4. Calibrated flow model based on distribution of heads in local wells over time. <p>It was assumed that the TCE concentrations in TA-V groundwater are no higher than 30 $\mu\text{g/L}$, which is reasonable given the maximum historical observed concentrations (see Section 2.3 of the CMI Plan).</p>
Dispersion	<p>Dilution and dispersion have contributed to the current distribution of TCE in TA-V groundwater. Dispersion will continue to affect TCE concentrations. A commonly used method for estimating longitudinal dispersivity is by applying the following empirical equation:</p> $\alpha_L = 3.28 * 0.83(\log_{10}(L_p / 3.28))^{2.414}$	<p>In this equation, α_L is the longitudinal dispersivity in feet, and L_p is the length of the plume in feet (Xu & Eckstein 1995). Transverse dispersivity (α_T) in feet can also be estimated by the following equation (ASTM 1995):</p> $\alpha_T = 0.33\alpha_L$

C-2.1 Model Domain

The model domain represents an area larger than TA-V in order to establish a subregional flow field through the alluvial fan deposits (Figure C-1) within which the local area of TA-V could be refined. The model grid is refined within TA-V in order to increase resolution in that area. Grid boundaries were specified head and no-flow boundaries based on observed water levels in four wells. The grid encompasses a total of approximately 6 mi² and consists of 94 rows and 74 columns. Cell sizes vary from approximately 50 ft on a side within TA-V to approximately 500 ft on a side at more distant areas (Figure C-1). A single layer represents the uppermost 50 ft of the groundwater system and is oriented parallel to the potentiometric surface at the beginning of the flow simulation (1993).

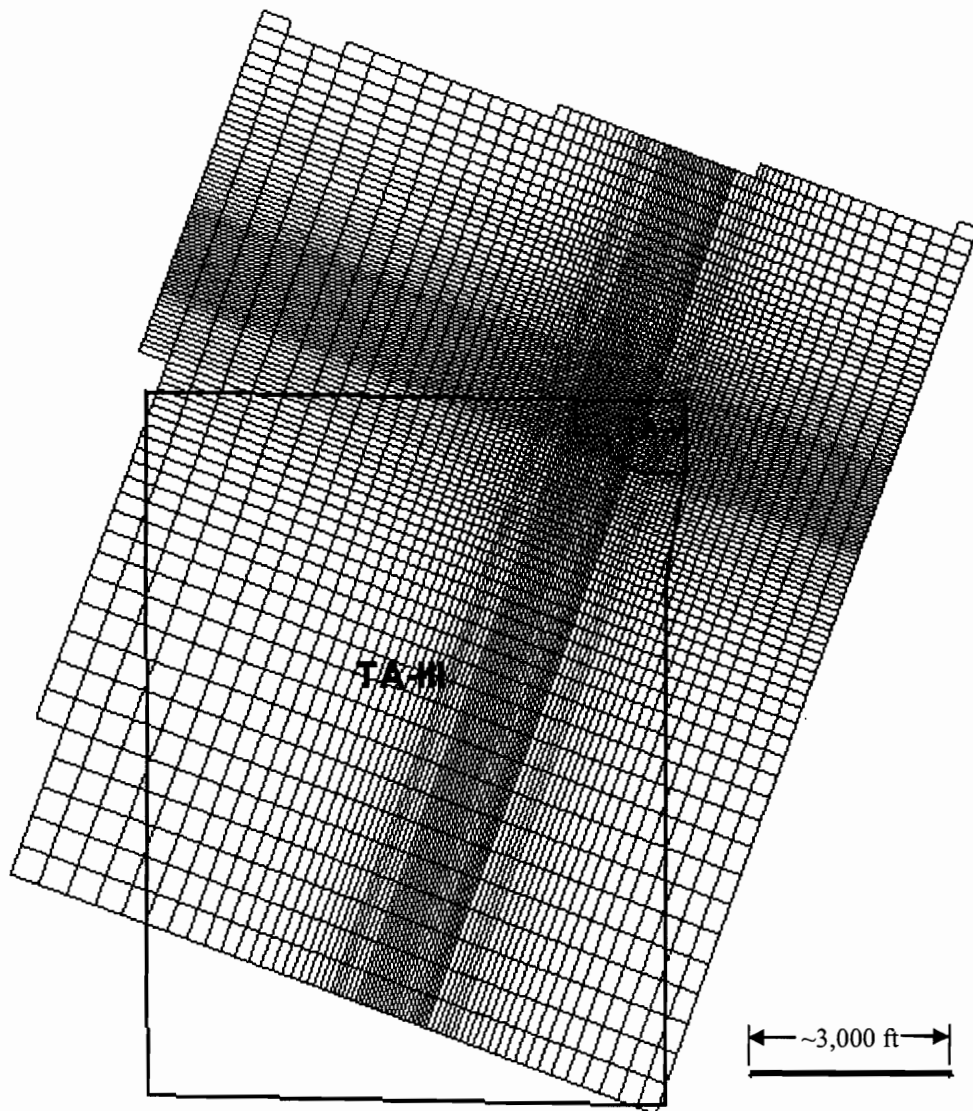


Figure C-1. Model grid illustrating model boundaries and discretization.

C-2.2 Model Calibration

Two data sets were used to calibrate the groundwater flow and transport model, as follows:

1. Measured water levels in 15 groundwater monitoring wells from 1993 to 2006, and
2. TCE concentration data, as measured using conventional sampling methods from 2001 to 2005.

Two numerical simulations were run for calibration. The first simulation began in 1993 and was used exclusively to calibrate the flow model to the observed water levels, and the second simulated TCE transport into the future using the calibrated flow model.

An automated parameter estimation approach was used to calibrate the flow model to observed water levels by varying the horizontal hydraulic conductivity, which was restricted to a range of 0.01 to 35 ft/day based on the conceptual model described in Table C-1. The resulting horizontal hydraulic conductivity distribution is illustrated in Figure C-2. This distribution reflects a relatively low hydraulic conductivity zone at TA-V. Appendix A contains plots of observed hydraulic head in the 15 wells located in the model domain. These wells and the simulated potentiometric surface are shown on Figure C-3. Potentiometric surface and water levels are expressed in feet above mean sea level (ft-amsl). Simulated water levels in all of these wells were generally within 1 ft of the observed water level over the simulated time period. Those few measured water levels that differ from simulated water levels by more than 1 ft do not appear to follow the general trend of the measured water levels over time and are considered anomalous.

The calibrated flow model was then used as the basis for simulating TCE transport using MT3DMS. Transport parameter input and assumptions are described in Table C-1. Calibration of the transport model to observed TCE concentrations in the period from 2001 to 2005 was performed by manually varying the initial TCE concentrations assigned based on the location of historical sources and measured concentrations in 2001. The resulting simulated concentrations were then compared to observed concentration data, and the starting concentrations were iteratively modified to arrive at a reasonable simulation of the observed concentration trends. Observed and final predicted TCE concentrations in six wells are shown in Appendix B. The flow and transport simulation ends in the year 2050 when water levels are predicted to fall below the bottom of the simulation layer in some cells as a result of regional water level declines caused by continued groundwater extraction for municipal supply.

DRAFT

Shading represents horizontal hydraulic conductivity according to the following scale:

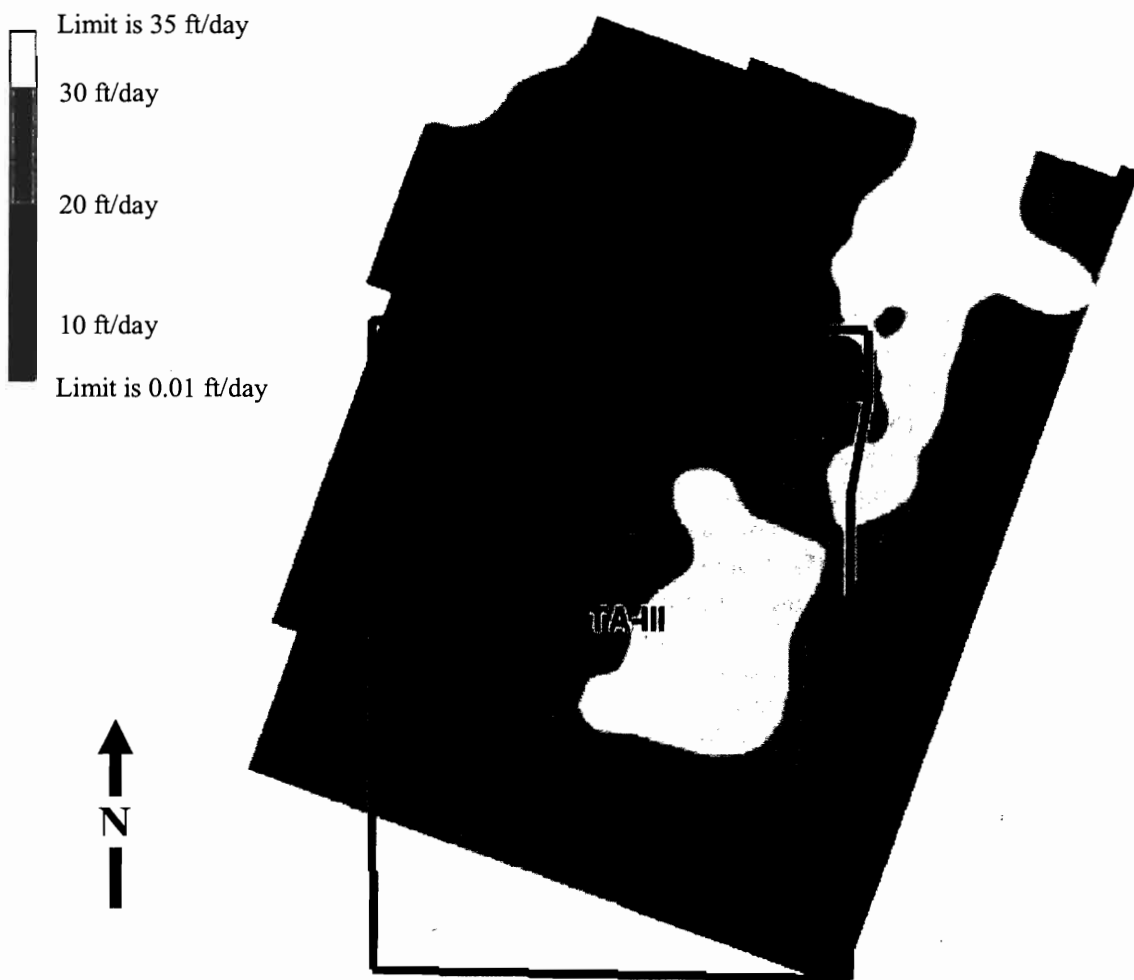
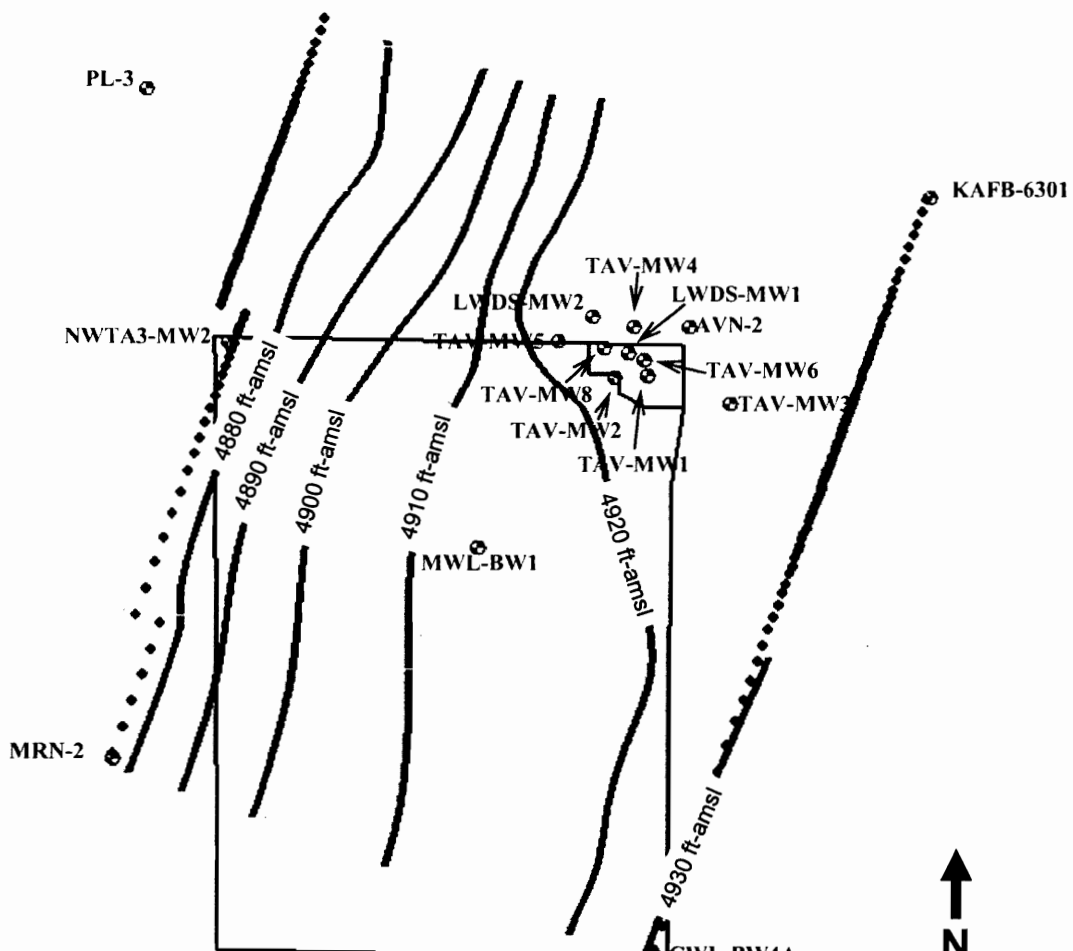


Figure C-2. Simulated hydraulic conductivity distribution.

DRAFT



LEGEND

- Monitoring well used for flow model calibration
- ◆ Specified head cell
- Potentiometric surface contour

Figure C-3. Simulated potentiometric surface in 2006.

C-3 RESULTS AND INTERPRETATION

The calibrated flow and transport model was used to simulate flow and transport under three scenarios using the average degradation rate constant as well as the upper and lower 95% confidence limits. The results are included in Appendix B and presented in this section.

C-3.1 Local Groundwater Flow Characteristics

The rate and direction of groundwater flow within and near TA-V will control changes in plume contours and plume migration during the implementation of the MNA remedy. It is important to understand both regional and local groundwater flow patterns in order to understand the potential for plume migration and plume contour dynamics.

The numerical model simulated flow through the alluvial fan/piedmont deposits within and around TA-V incorporating the effects of mountain front recharge and municipal groundwater withdrawal. This groundwater flowed to the west at a rate similar to the rate simulated in previous regional modeling activities (Section C-2). As previously stated, this system is characterized by declining water levels.

The model grid was more finely discretized in the TA-V area to provide resolution in simulated groundwater flow and transport in that area. The aquifer at TA-V has lower hydraulic conductivity than in much of the surrounding area. Groundwater flow at TA-V is primarily governed by a local low hydraulic conductivity zone. As regional water levels decline (effectively draining the alluvial fan deposits), the local low hydraulic conductivity zone at TA-V drains more slowly than surrounding areas. This results in a residual groundwater mound and local flow lines that are often in a direction counter to the subregional direction. This effect is shown in simulated flow vectors from the year 2001, as shown on Figure C-4. The low hydraulic conductivity zone around TA-V will also result in groundwater flow velocities that are slower at TA-V than in the surrounding aquifer.

The predicted result of this local flow pattern is contaminant transport in several directions at a much slower rate than under the subregional flow conditions. Based on this flow model, the future TCE plume dynamics were predicted as described in Section C-3.2. It is anticipated that TCE plume migration or expansion will be limited by degradation.

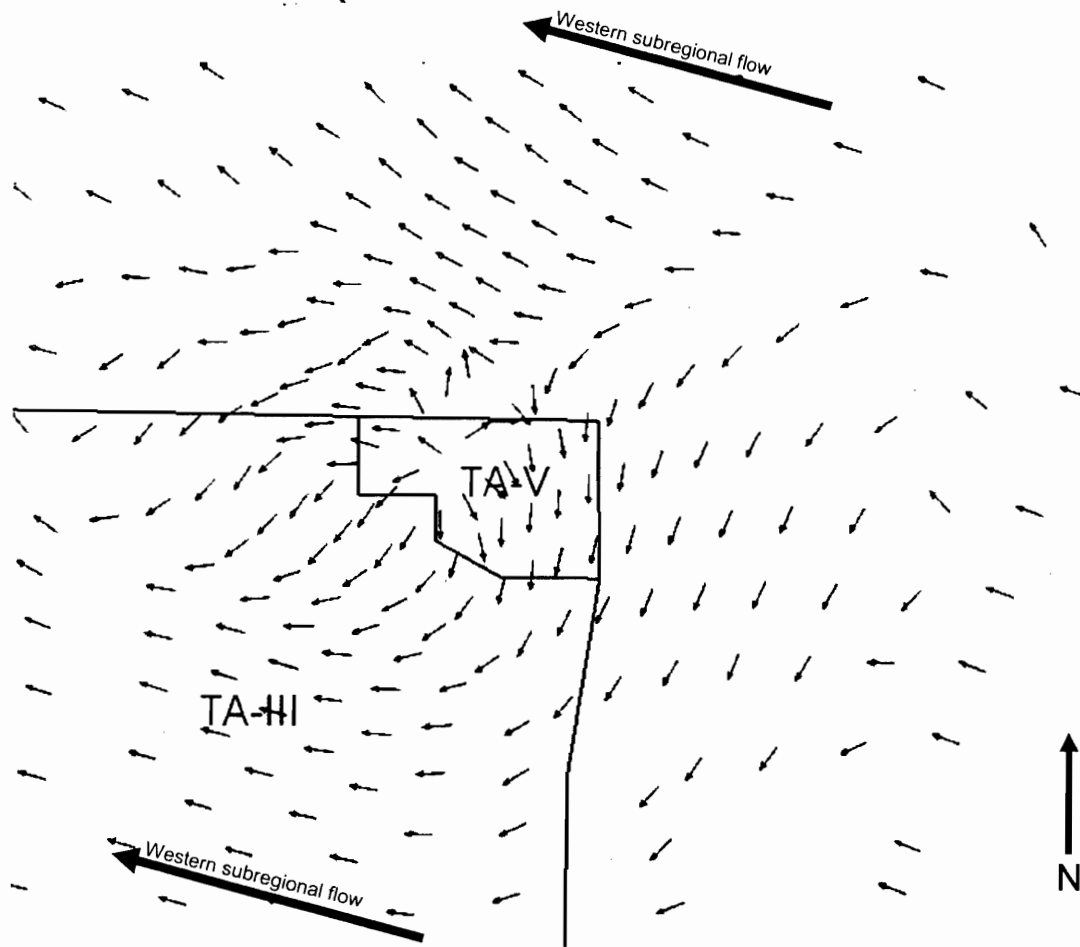


Figure C-4. Simulated groundwater flow vectors near TA-V (2001).

C-3.2 Future TCE Plume Dynamics

Figures C-5 through C-7 are simulated TCE concentration isopleths for the average and two 95% confidence limits of the degradation rate constant. Each of these figures shows simulated TCE concentrations corresponding to three time periods. These three time periods correspond to:

1. **Current conditions**—the current simulated plume distribution (2006),
2. **The highest simulated concentrations in selected wells**—an intermediate time period during which the maximum concentration of TCE occurred in wells TAV-MW6 and TAV-MW1, and
3. **Simulated result of natural attenuation**—In the case of the average and the fastest degradation rate (the upper 95% confidence limit of the degradation rate constant), the third time period is the year after which TCE concentrations were predicted to be below 5 $\mu\text{g/L}$; this occurred in the years 2049 and 2032, respectively. In the case of the slowest degradation rate (the lower 95% confidence limit of the degradation rate constant), the simulation was run until 2050, at which time some TCE concentrations remained above 5 $\mu\text{g/L}$ at the end of the simulation. In the year 2050, the simulation was halted due to regionally declining water levels and subsequent dewatering of the model domain.

DRAFT

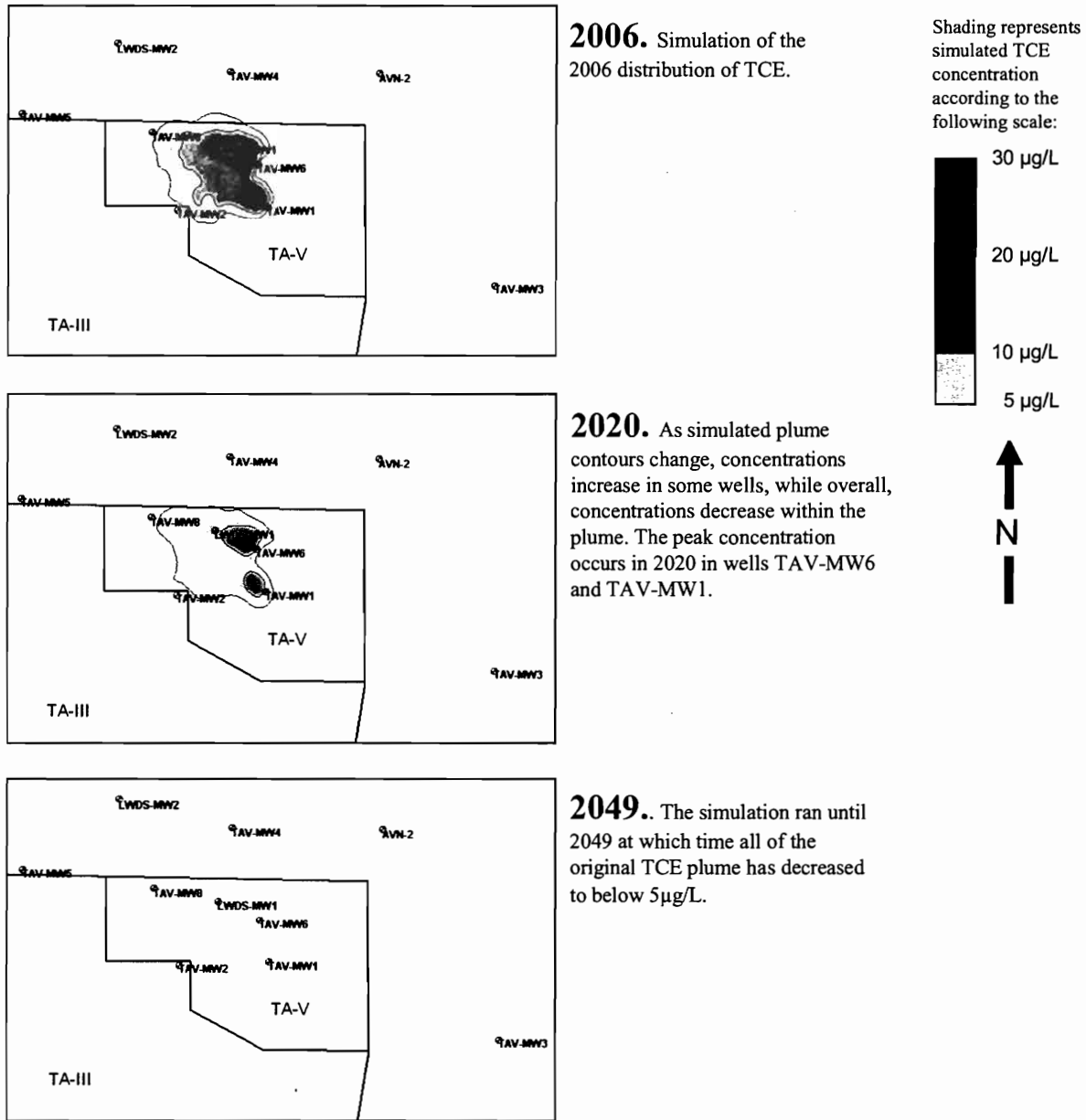


Figure C-5. Simulated TCE concentration contours using the average degradation rate constant.

DRAFT

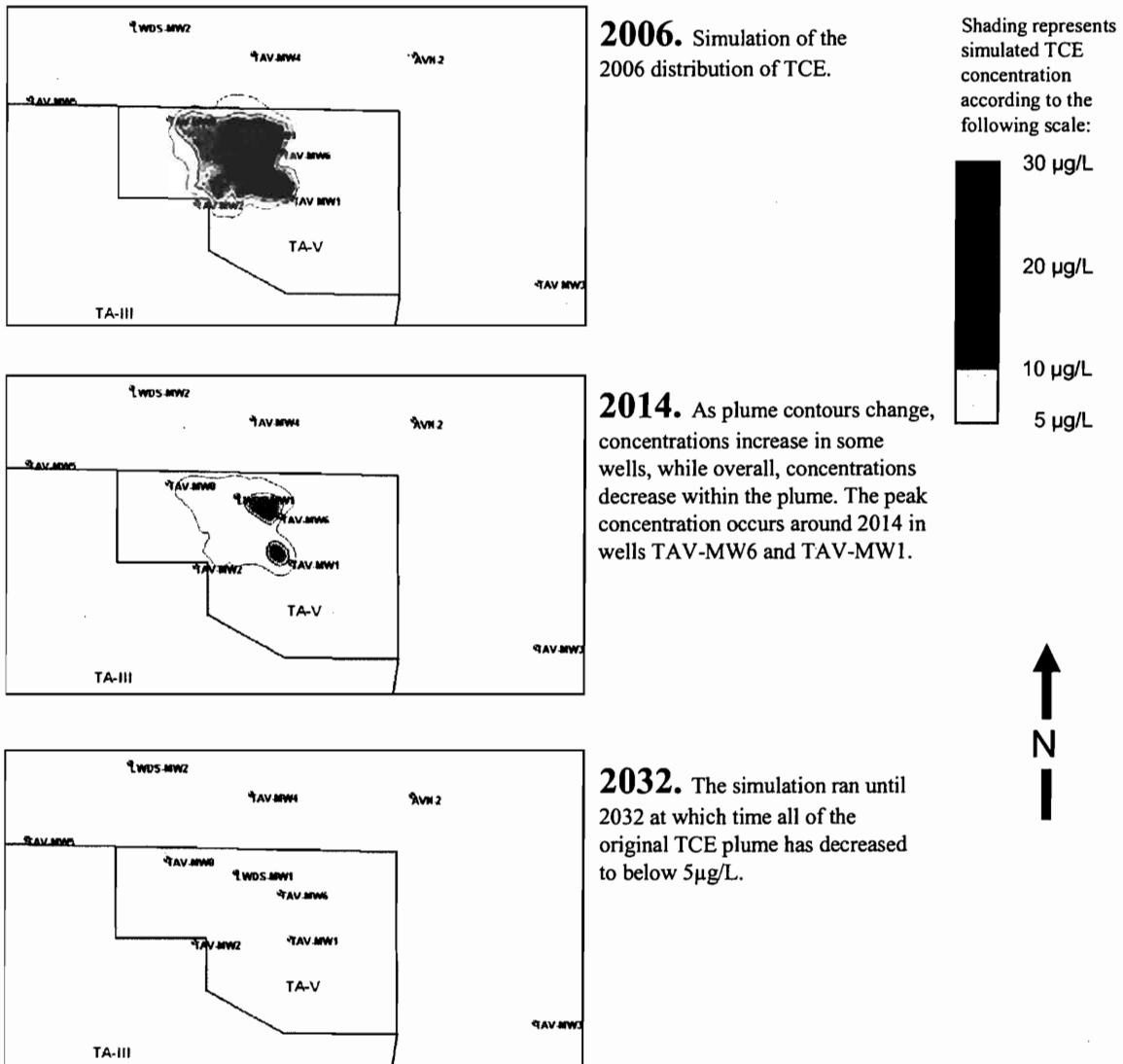
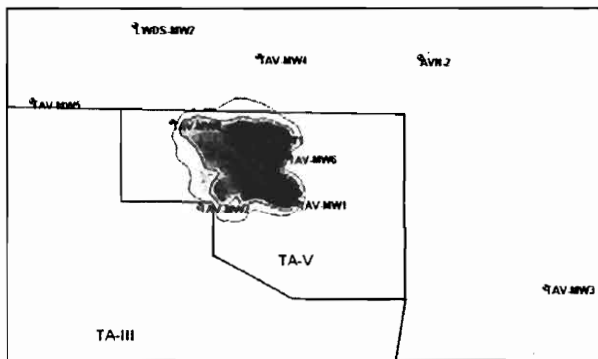


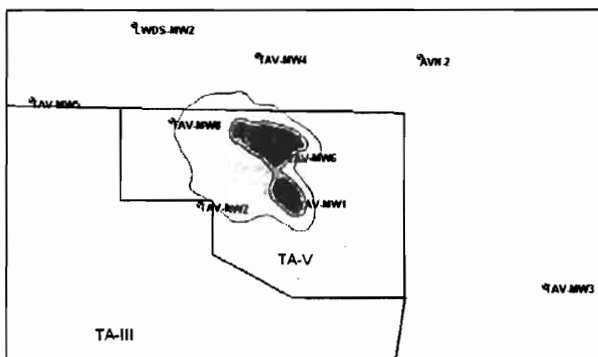
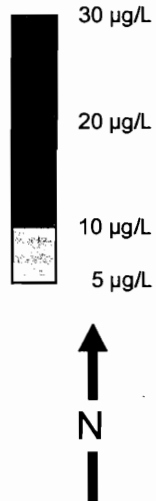
Figure C-6. Simulated TCE concentration contours using the upper 95% confidence interval of the degradation rate constant.

DRAFT

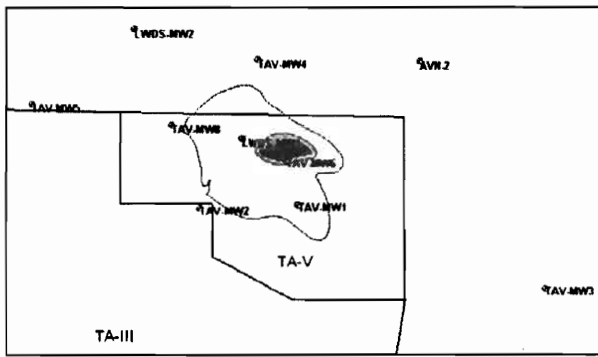


2006. Simulation of the 2006 distribution of TCE.

Shading represents simulated TCE concentration according to the following scale:



2031. As plume contours change, concentrations increase in some wells, while overall, concentrations decrease within the plume. The peak concentration occurs around 2031 in wells TAV-MW6 and TAV-MW1.



2050. The simulation ran until 2050, and was terminated due to cell drying. Plume concentrations decrease, but a greater than 5 $\mu\text{g/L}$ plume remains.

Figure C-7. Simulated TCE concentration contours using the lower 95% confidence interval of the degradation rate constant.

DRAFT

Observations and interpretation from the model output are as follows:

- The direction and rate of TCE migration are strongly influenced by the local radial flow pattern caused by the relatively low hydraulic conductivity at TA-V, and therefore some TCE migration does not coincide with the westerly subregional groundwater flow direction.
- TCE concentrations will decline over time throughout the plume as a whole due to dispersion and degradation (Figures C-5 through C-7). Nevertheless, TCE concentrations at some wells are predicted to increase over the next several years (Appendix B) as groundwater with higher TCE concentrations migrates from upgradient of these wells. For example, peak TCE concentrations at TAV-MW1 and TAV-MW6 (simulated using the average rate constant) are predicted to occur in the year 2020 followed by a decrease in TCE concentrations.
- Over the course of the model simulation, the highest TCE concentrations remained within the area sampled by the TA-V monitoring well network.

The CMI model is based on several assumptions. For instance, it was assumed that the maximum concentration of TCE in TA-V groundwater is less than 30 µg/L. This is reasonable given the historical maximum concentration; nevertheless, it is an assumption in regards to regions between monitoring wells. Therefore, the model should not be used exclusively to predict concentrations at specific wells and times without considering the uncertainty associated with this assumed starting concentration. The model is intended to illustrate the general trends of the TCE plume at TA-V, including dynamics of plume contours, potential for migration, and the effects of natural attenuation.

C-3.3 Achieving Cleanup Goals

As stated in Section 3.2 of the CMI Plan, one of the compliance objectives for the MNA remedy is to reduce COC concentrations throughout the plume to below cleanup goals (MCLs) for eight consecutive quarters. An estimate of when this goal will be achieved is provided here using the modeling results. This estimate is provided in keeping with United States Environmental Protection Agency (EPA) guidance (EPA 2004), which states that the EPA:

“...recognizes the uncertainties associated with the cleanup may make it impossible to specify with a high level of confidence when a remedy will achieve final cleanup goals . . . facilities should generally still attempt to predict the time needed to achieve final cleanup goals, but stakeholders should recognize that such predictions are best considered in a relative sense for comparing one cleanup option to another. EPA recommends that cleanup timeframes primarily focus on the schedules associated with implementing the remedy.”

DRAFT

The uncertainties associated with this estimation must be considered when applying the results to the CMI.

The estimated time needed to achieve cleanup goals is primarily governed by the reduction in TCE concentration by natural attenuation processes until TCE concentrations are below 5 µg/L. Natural attenuation processes simulated in the numerical model include dispersion and biological degradation. As described, three simulations were run corresponding to the average and the upper and lower 95% confidence limits of the degradation rate constant.

The times presented here correspond to the predicted time at which all simulated TCE concentrations are below the cleanup goal of 5 µg/L. This cleanup goal is estimated to be reached in the year 2049 using the average degradation rate constant. The cleanup goal is estimated to be reached in the year 2032 using the upper 95% confidence limit of the degradation rate constant.

However, at the end of the simulation (2050), some TCE concentrations remained above the cleanup goal in the simulation using the lower 95% confidence limit of the degradation rate constant. The year in which the cleanup goal will be achieved according to the lower 95% confidence limit was predicted by extrapolation. The maximum TCE concentration observed in any of the model cells at the end of the simulation was 13.1 µg/L. The estimated additional time until TCE concentrations fell to 5 µg/L by degradation was calculated using the first-order degradation rate equation solved for time (t), as follows:

$$t = \frac{\ln\left(\frac{C}{C_0}\right)}{-k_1}$$

where

t = time (days) required for concentration to decline from C_0 (13.1 µg/L) to C (5 µg/L),
C = target concentration of 5 µg/L,
 C_0 = maximum concentration at the end of the model run (13.1 µg/L), and
 k_1 = the lower 95% confidence limit of the first-order degradation rate constant, which is the average rate plus the 95% confidence interval.

The estimated additional time (70 years) was added to the length of model run (2050) to arrive at the estimated cleanup date for the lower 95% confidence (2120). This approach does not take dispersion into account, which would cause concentrations to decline more rapidly.

DRAFT

C-4. IMPLICATIONS FOR CORRECTIVE MEASURES IMPLEMENTATION

The CMI model provides a representation of future TCE plume dynamics at TA-V on a local scale in support of the MNA implementation strategy. The simulation provides a general representation of natural attenuation processes with several implications that have guided the development of the MNA implementation strategy. These implications include:

- **Action levels developed using the CME modeling results are conservative.** The CME model intentionally neglected some contaminant reducing processes, which include degradation and dispersion, in order to be conservative. These contaminant reducing processes were not neglected in the local-scale CMI model. The results of the less conservative CMI model suggest that TCE concentrations will be reduced more quickly and that the action level is conservative.
- **TCE plume dynamics will include a short-term concentration increase in some wells followed by a decrease in concentrations in all wells.** The modeling results illustrate that over the short term (i.e., approximately 8 to 25 years) concentrations in some wells may increase. This increase may occur in directions that are counter to the regional flow lines due to local heterogeneities. Eventually, concentrations will decline as natural attenuation processes decrease the overall concentration of TCE within the plume. The results illustrate that the overall TCE mass within TA-V groundwater is decreasing due to intrinsic degradation. Eventually, TCE concentrations, as observed in samples from all wells, will decrease until cleanup goals are achieved.
- **The TCE plume is not predicted to move beyond the monitoring well network.** The TCE plume will not migrate away from the current monitoring wells and will not migrate to production wells. In general, natural attenuation processes will act to decrease TCE concentrations before significant migration can occur. Locally at TA-V, groundwater flow rates are slow relative to the subregional flow field. Water levels in TA-V monitoring wells should be measured to monitor potential changes in hydraulic conditions as water levels within the aquifer decline.
- **Cleanup goals will be achieved within a reasonable timeframe.** The timeframe of remedy implementation is governed by natural attenuation processes that decrease the concentration of TCE. The numerical modeling results suggest that the natural attenuation processes will decrease TCE concentrations to below cleanup goals sometime between the years 2032 and 2120. This timeframe is reasonable considering the plume dynamics simulated in the CMI model and the conservatively estimated travel time to potential receptors (SNL/NM 2005).

C-5. REFERENCES

ASTM, 1995, "Standard Guide for Risk-Based Corrective Action Applied at Petroleum Release Sites," ASTM E-1739-95, American Society for Testing and Materials, Philadelphia, PA.

Bexfield, L.M., and D.P. McAda, 2003, "Simulated effects of ground-water management scenarios on the Santa Fe Group Aquifer System, Middle Rio Grande Basin, New Mexico, 2001-40," U.S. Geological Survey Water-Resources Investigations Report 03-4040, 39 p.

BYU, 2003, "Department of Defense Groundwater Modeling System, Version 4.0," developed by the Environmental Modeling Research Laboratory at Brigham Young University for the U.S. Department of Defense, Army Corps of Engineers Waterways Experiment Station, Vicksburg, Mississippi. See <http://chl.wes.army.mil/software/gms> and <http://www.emrl.byu.edu/gms.htm>.

EPA, 2004, "Handbook of Groundwater Protection and Cleanup Policies for RCRA Corrective Action," EPA530-R-04-030, April 2004, <http://www.epa.gov/correctiveaction>, U.S. Environmental Protection Agency, Solid Waste and Emergency Response (5303W).

Harbaugh, A.W., E.R. Banta, M.C. Hill, and M.G. McDonald, 2000, *MODFLOW-2000, the U.S. Geological Survey Modular Ground-Water Model—User guide to modularization concepts and the ground-water flow process*, Open-File Report 00-92, U.S. Geological Survey, Branch of Information Services, Box 25286, Denver, CO 80225-0425 or http://water.usgs.gov/software/ground_water.html.

Ruskauff, Greg, 2004, "Modifications to and use of the Middle Rio Grande Model (WRIR 02-4200) for mixing analysis," Technical Memorandum to Sue Collins written November 10, 2004.

SNL/NM, 2001, "SNL/NM Environmental Restoration Project Long-Term Monitoring Strategy for Groundwater," Environmental Restoration Project, U.S. Department of Energy, Albuquerque Operations Office, Sandia National Laboratories/New Mexico, February 2001.

SNL/NM, 2004, "Current Conceptual Model of Groundwater Flow and Contaminant Transport at Sandia National Laboratories/New Mexico Technical Area-V," Sandia Report SAND2004-1470, April 2004.

SNL/NM, 2005, "Corrective Measures Evaluation Report for Technical Area-V Groundwater," Sandia Report SAND2005-5297.

Xu, M., and Eckstein, Y. 1995, "Use of weighted least-squares method in evaluation of the relationship between dispersivity and scale," *Groundwater*, 33(6), 905-908.

Zheng, C., and P.P. Wang, 1999, "MT3DMS, A Modular Three-Dimensional Multispecies Transport Model," U.S. Army Corps of Engineers, Strategic Environmental Research and Development Program (SERDP).

DRAFT

APPENDIX A

SIMULATED AND OBSERVED HEAD AT SELECTED WELLS

DRAFT

This Page Intentionally Left Blank

DRAFT

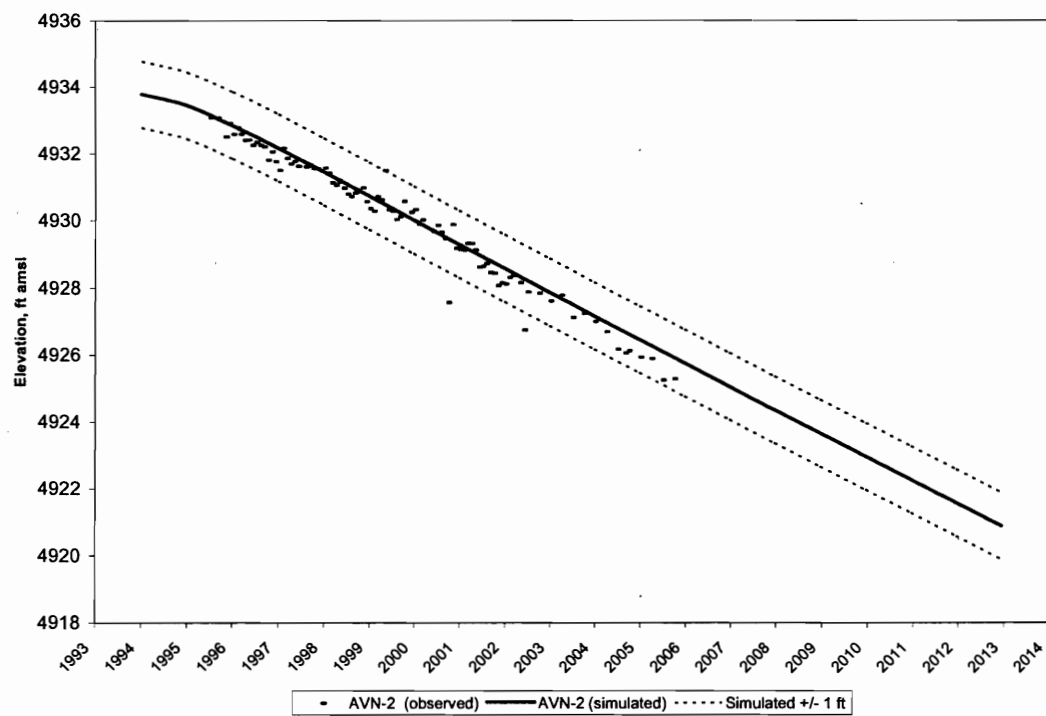


Figure A-1. Simulated and observed head in well AVN-2.

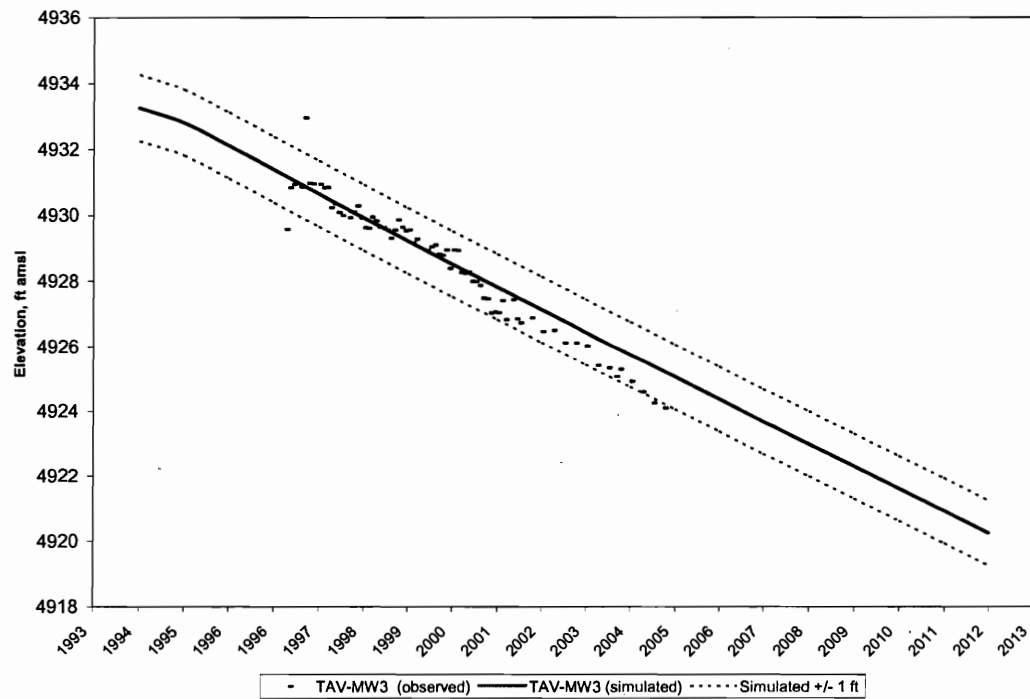


Figure A-2. Simulated and observed head in well TAV-MW3.



DRAFT

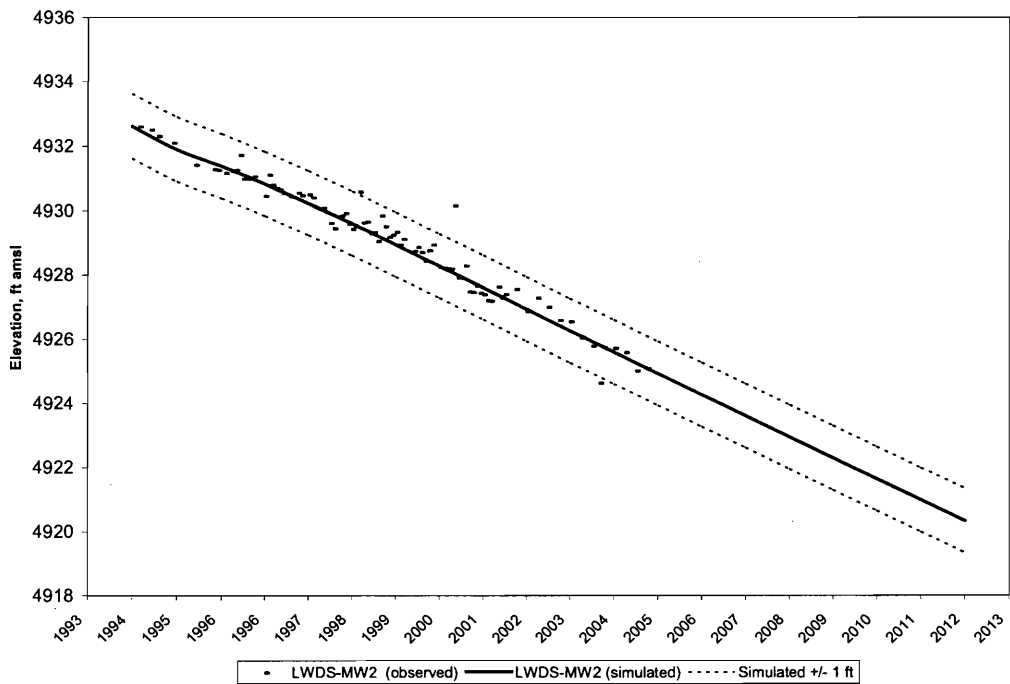


Figure A-3. Simulated and observed head in well LWDS-MW2.

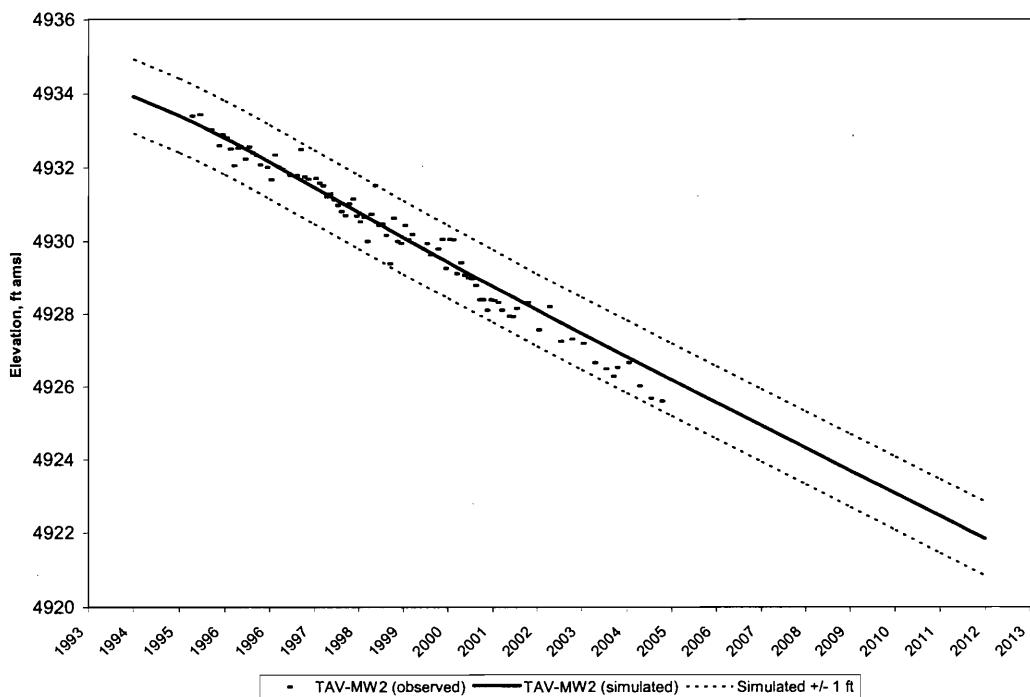


Figure A-4. Simulated and observed head in well TAV-MW2.

DRAFT

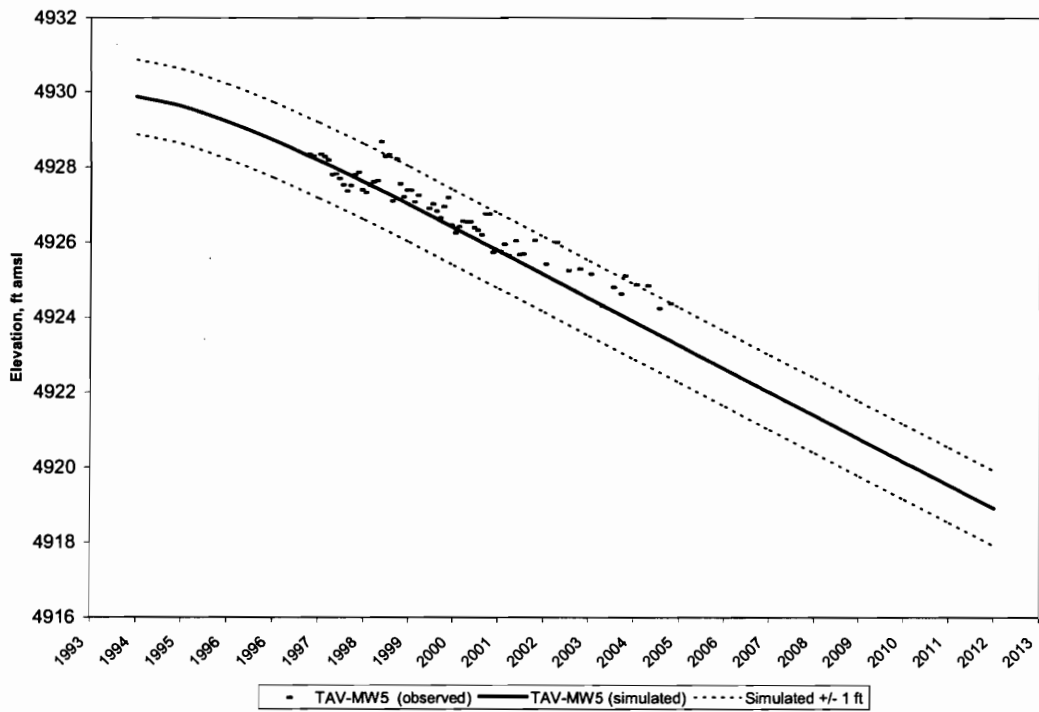


Figure A-5. Simulated and observed head in well TAV-MW5.

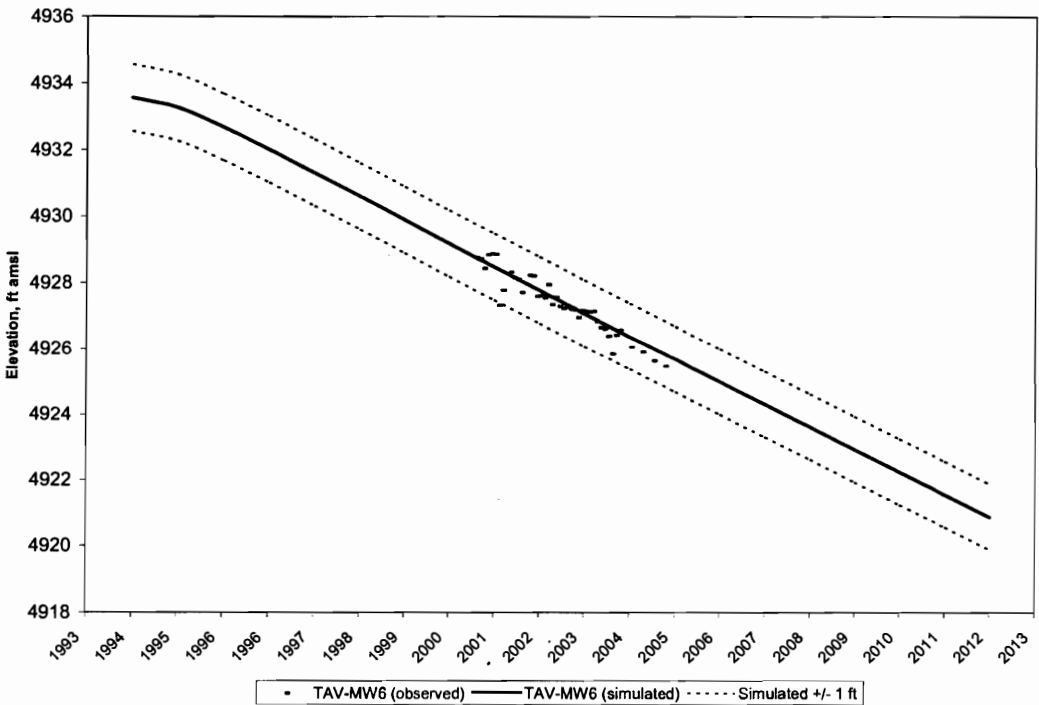


Figure A-6. Simulated and observed head in well TAV-MW6.

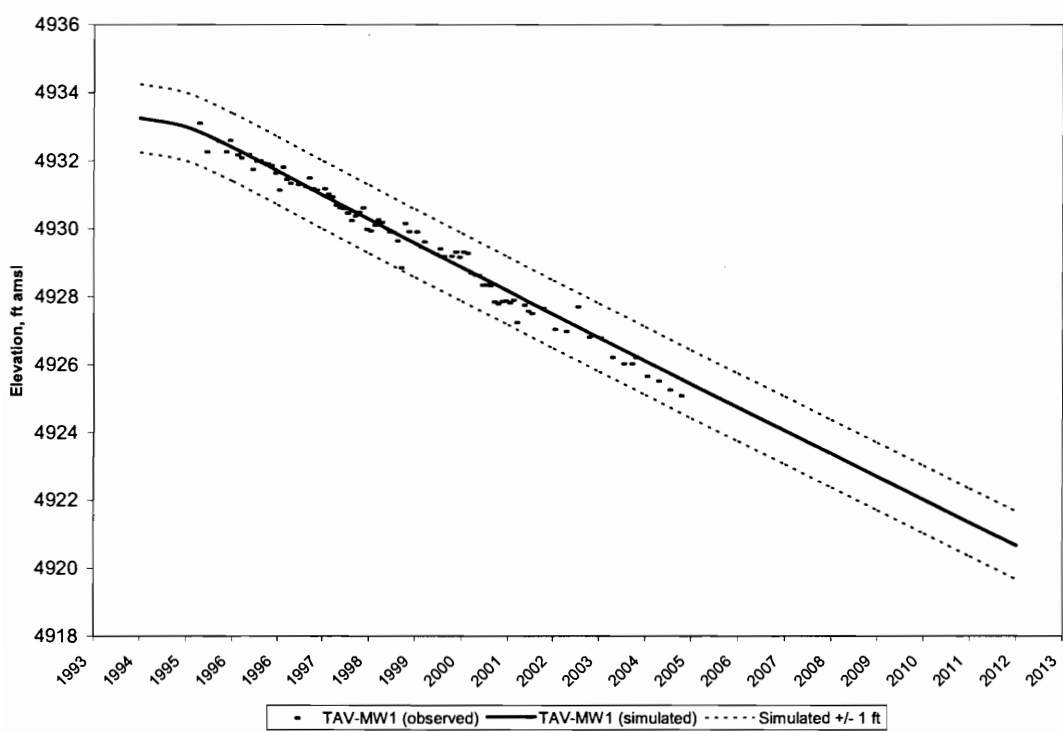


Figure A-7. Simulated and observed head in well TAV-MW1.

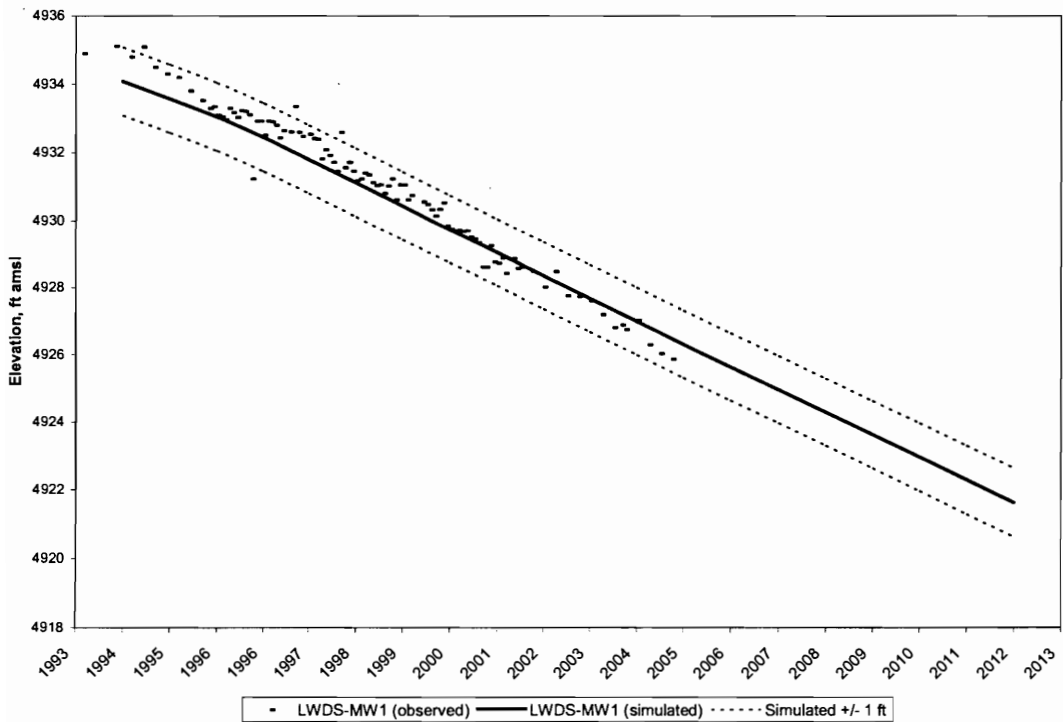


Figure A-8. Simulated and observed head in well LWDS-MW1.

DRAFT

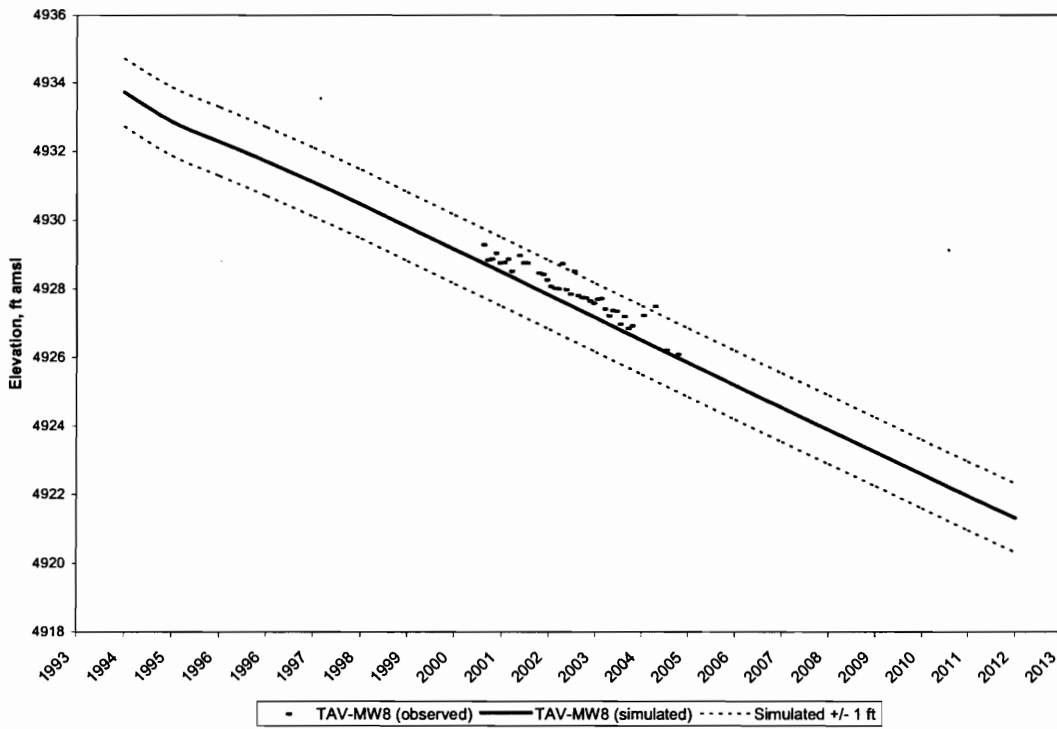


Figure A-9. Simulated and observed head in well TAV-MW8.

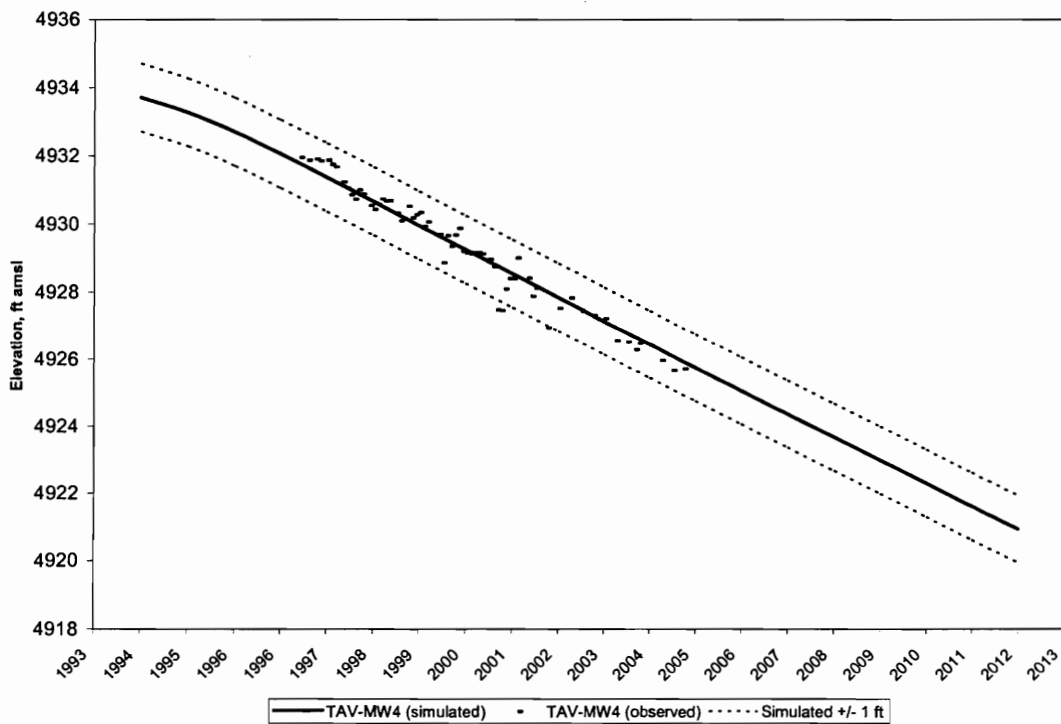


Figure A-10. Simulated and observed head in well TAV-MW4.

DRAFT

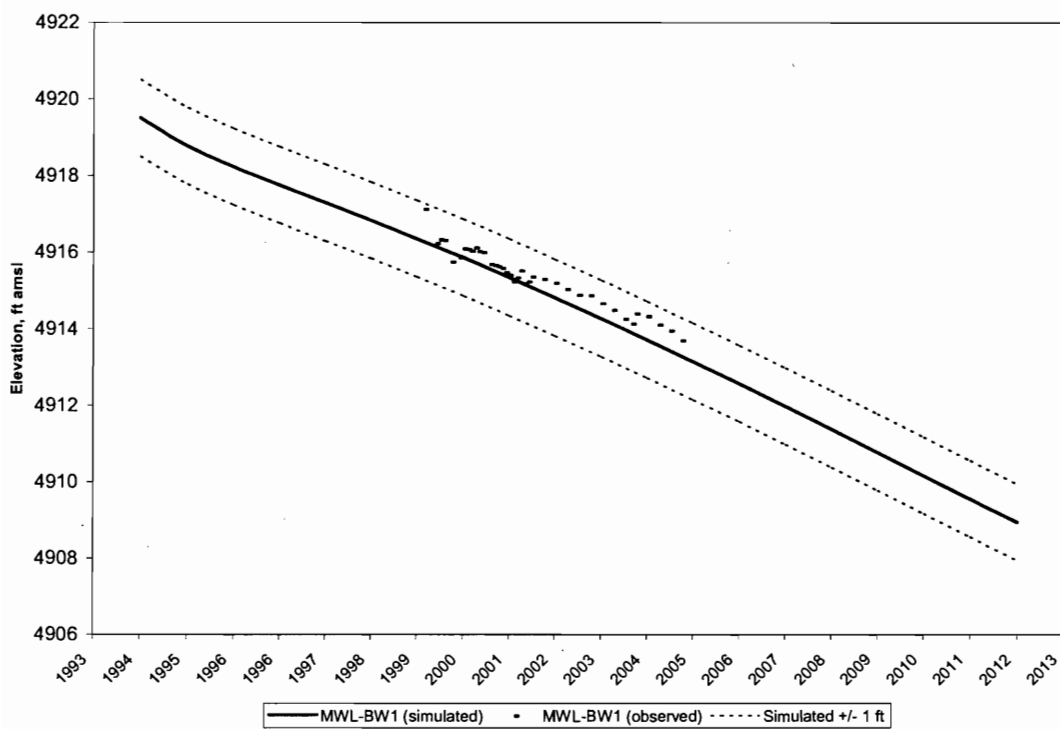


Figure A-11. Simulated and observed head in well MWL-BW1.

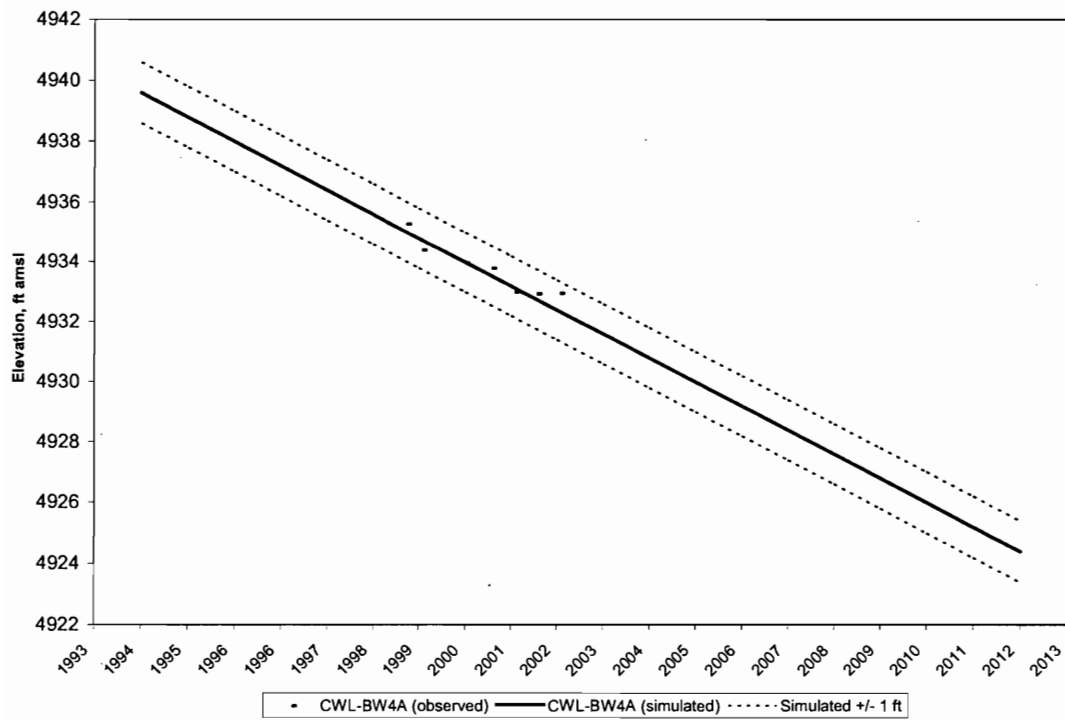


Figure A-12. Simulated and observed head in well CWL-BW4A.

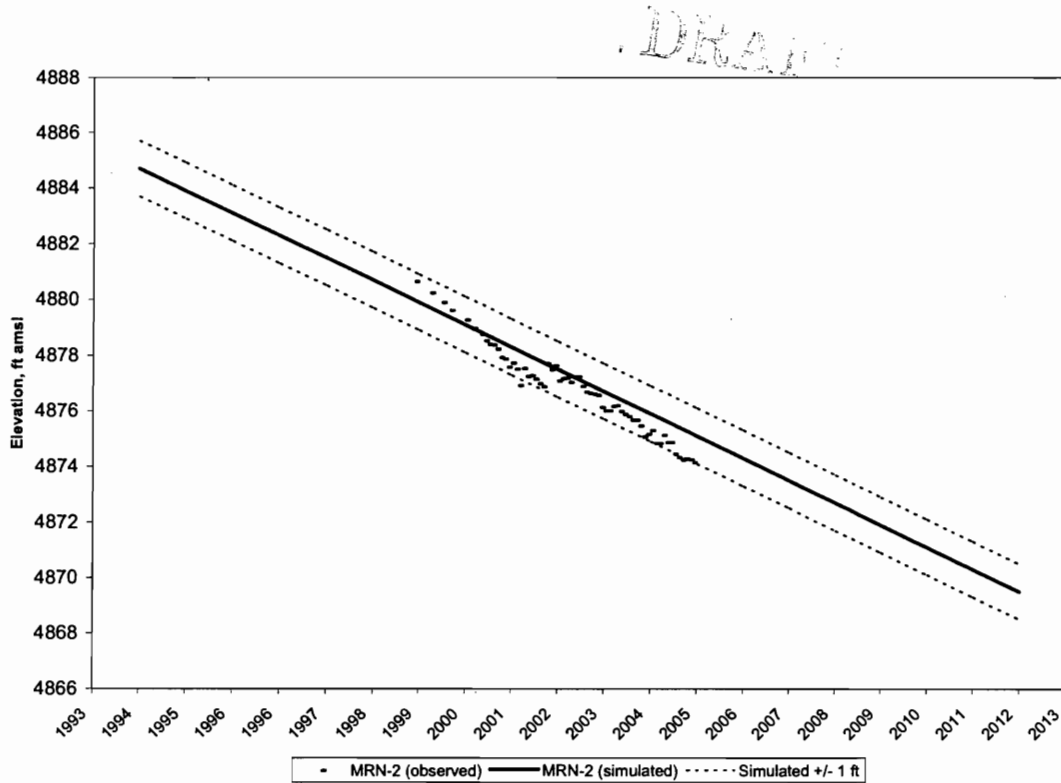


Figure A-13. Simulated and observed head in well MRN-2.

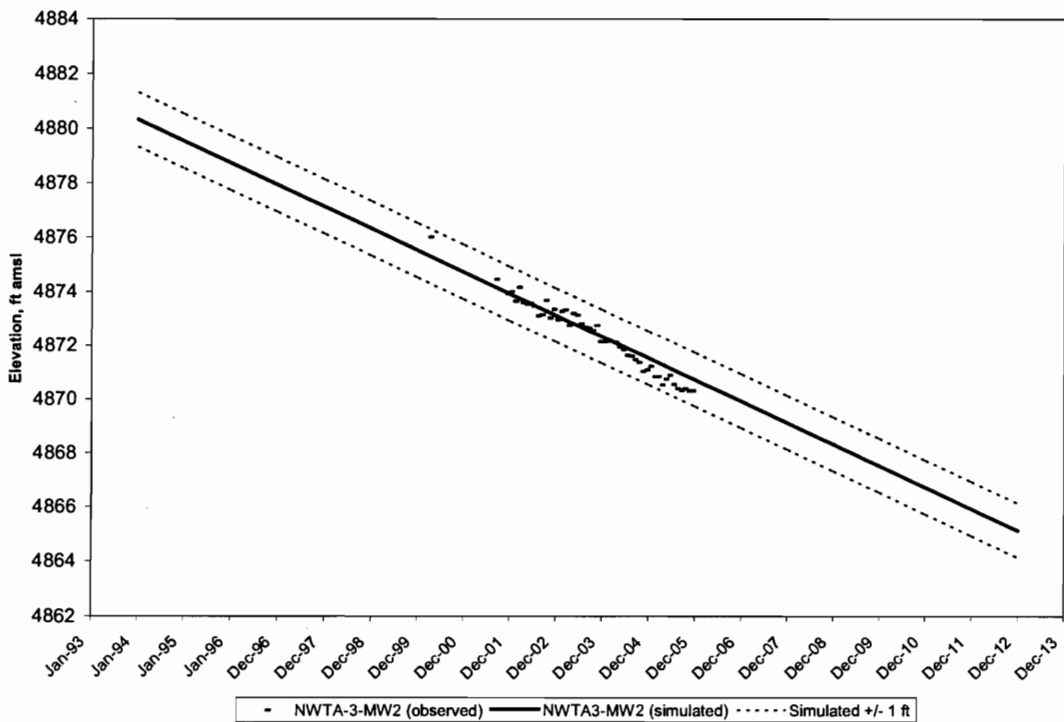


Figure A-14. Simulated and observed head in well NWTA3-MW2.

DRAFT

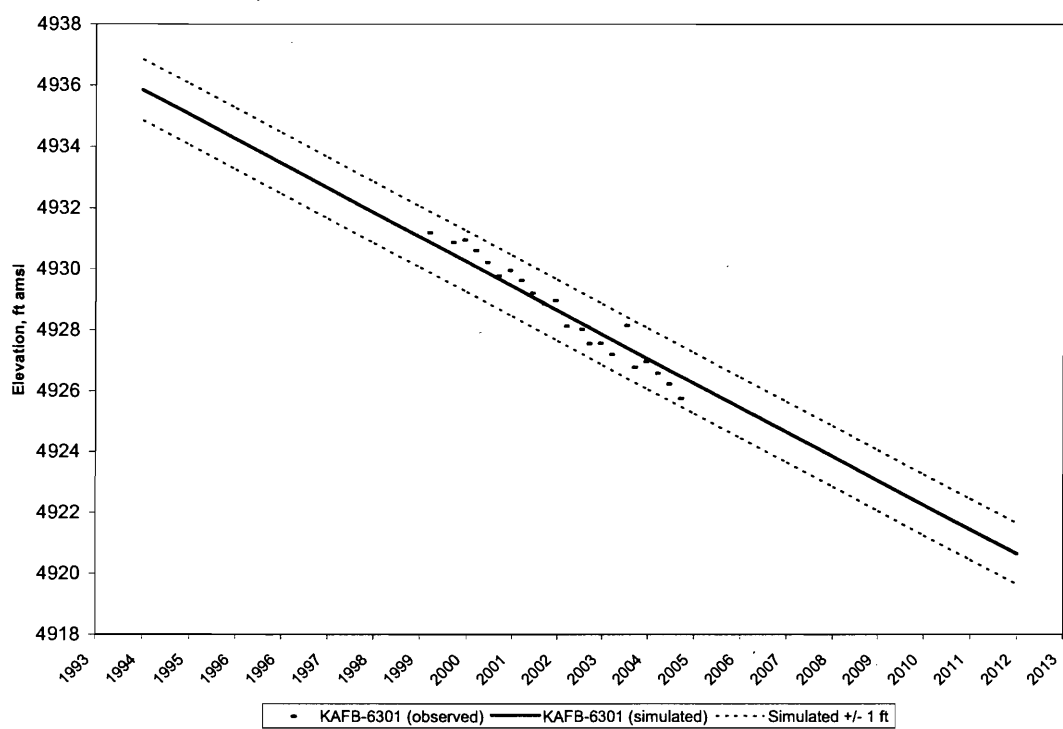


Figure A-15. Simulated and observed head in well KAFB-6301.

Draft

APPENDIX B

**SIMULATED AND OBSERVED TCE CONCENTRATIONS AT SELECTED
WELLS**

Diagram 1

This Page Intentionally Left Blank

DRAFT

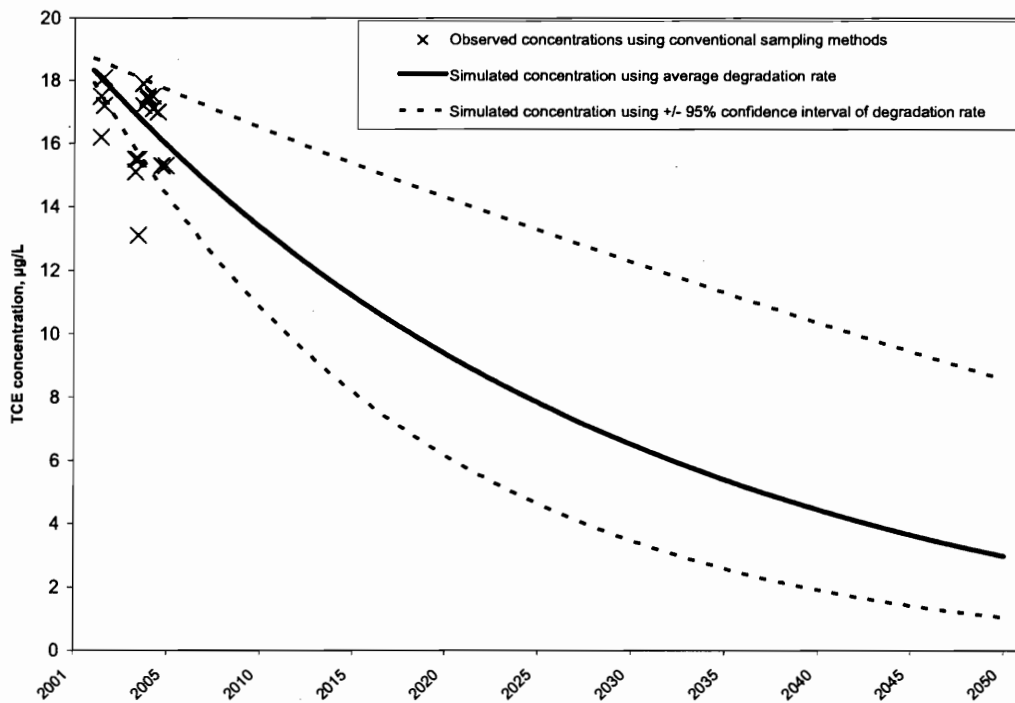


Figure B-1. Simulated and observed concentrations from well LWDS-MW1.

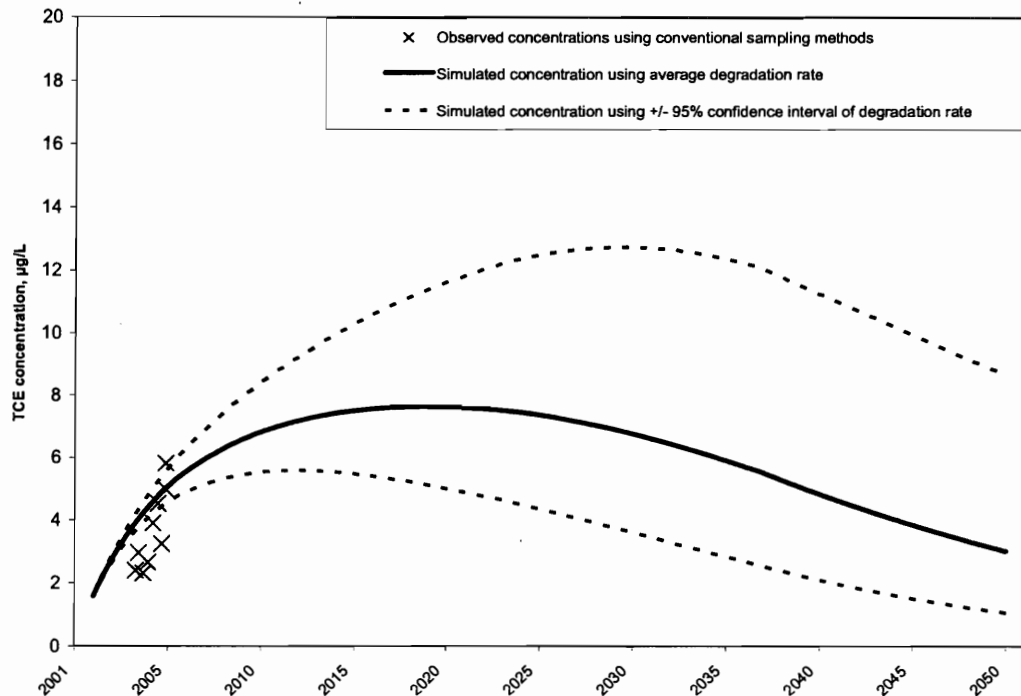


Figure B-2. Simulated and observed concentrations from well TAV-MW1.

DRAFT

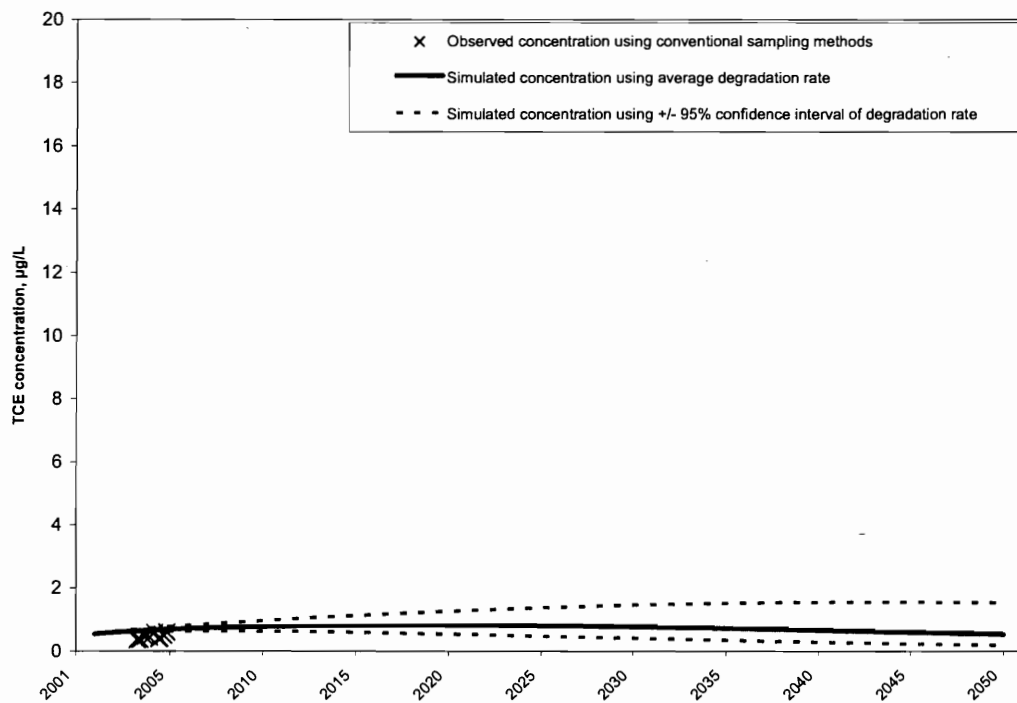


Figure B-3. Simulated and observed concentrations from well TAV-MW2.

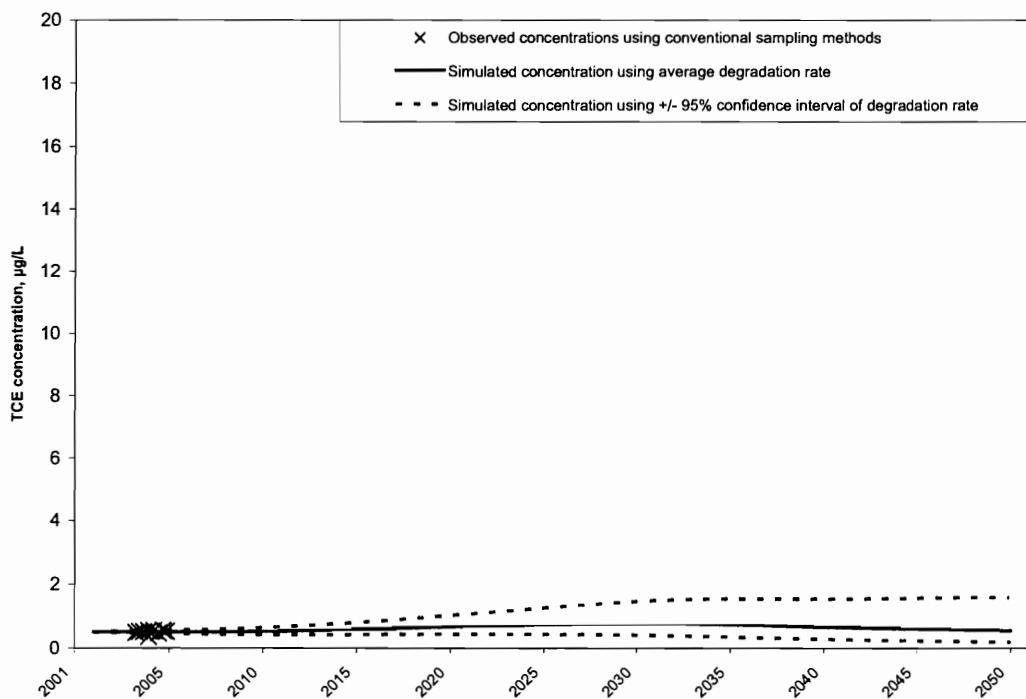


Figure B-4. Simulated and observed concentrations from well TAV-MW4.

DRAFT

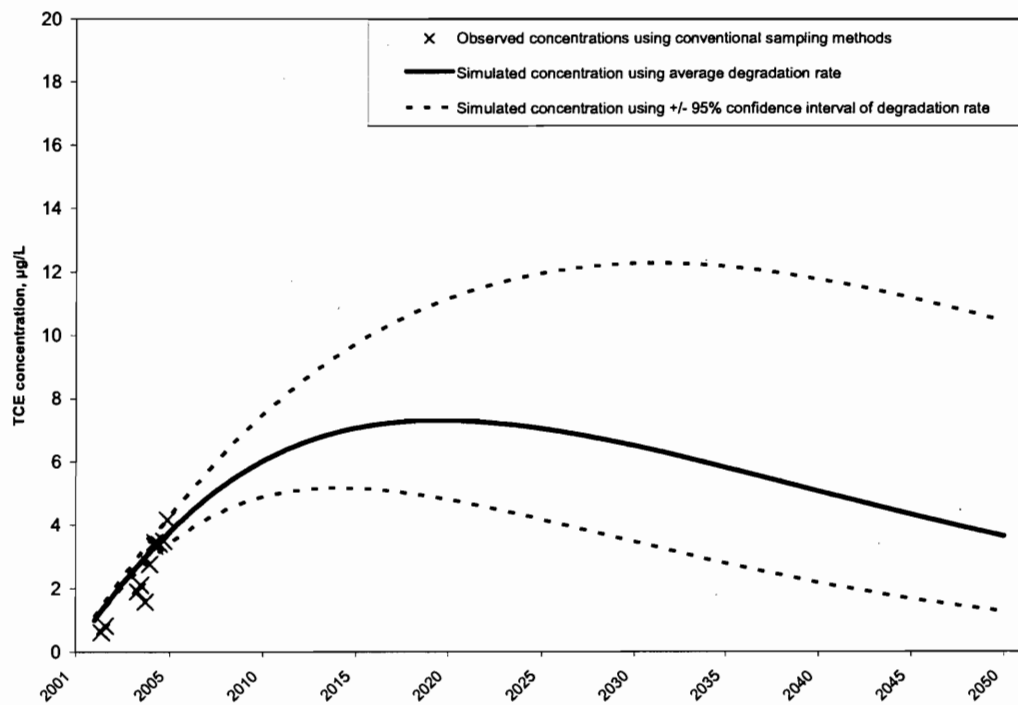


Figure B-5. Simulated and observed concentrations from well TAV-MW6.

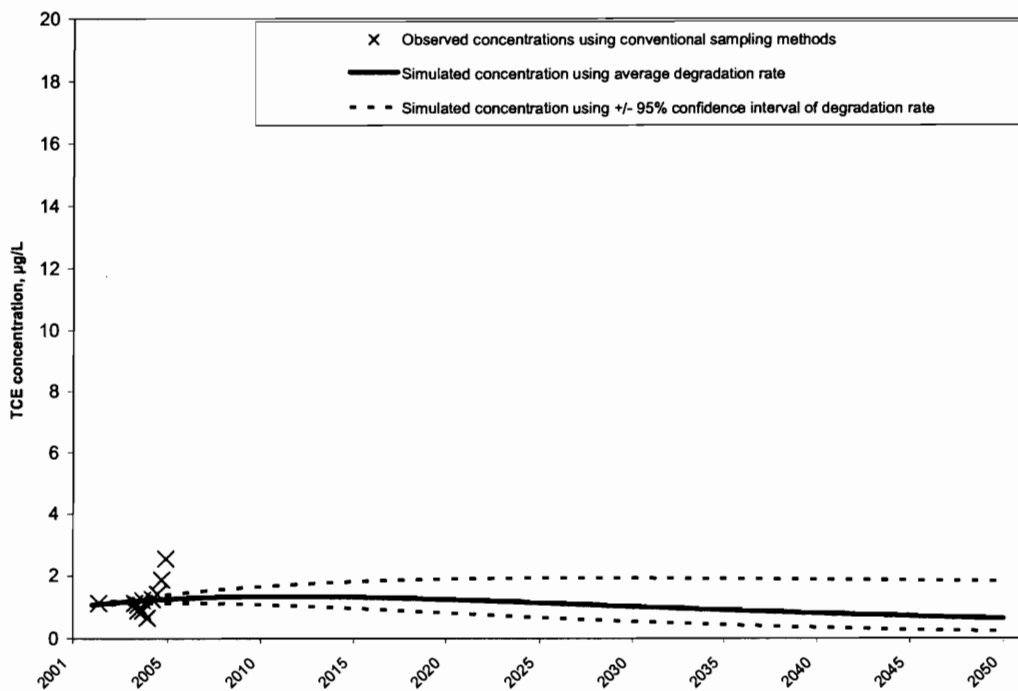
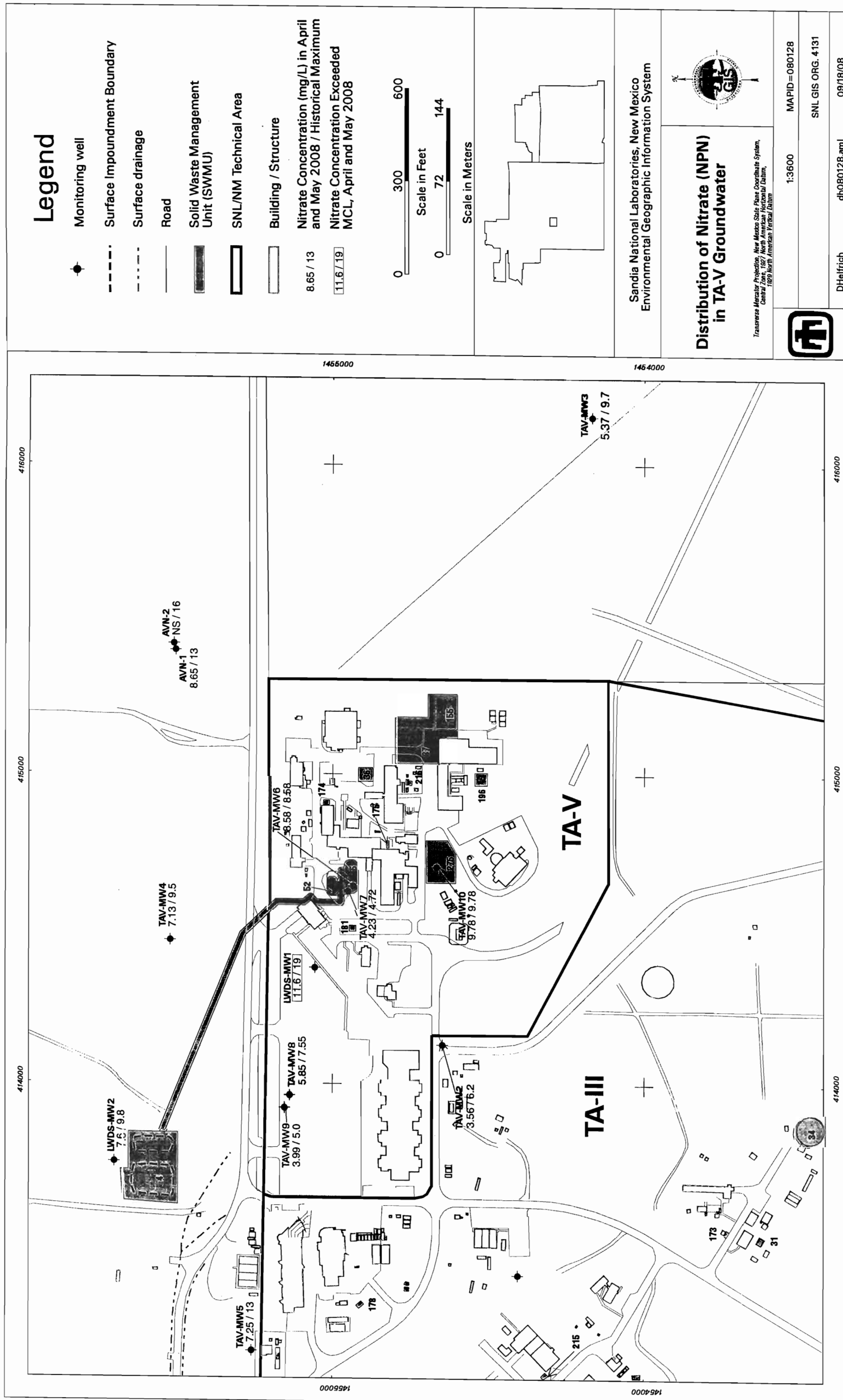


Figure B-6. Simulated and observed concentrations from well TAV-MW8.

This Page Intentionally Left Blank



NPN and Nitrate Concentrations in LWDS-MW1

